A METHOD TO CALIBRATE ANALYTICAL MODELS OF MULTI-STORY

BUILDINGS FROM EARTHQUAKE RECORDS

by

Sedef Kocakaplan

B.S., Civil Engineering, Kocaeli University, 2010

Submitted to Kandilli Observatory and Earthquake Research Institute

in partial fulfillment of the requirements for the degree of

Master of Science

Graduate Program in Earthquake Engineering

Boğaziçi University

2014

A METHOD TO CALIBRATE ANALYTICAL MODELS OF MULTI-STORY
BUILDINGS FROM EARTHQUAKE RECORDS

APPROVED BY:

Prof. Dr. Erdal Şafak …………………………...

(Thesis Supervisor)

Prof. Dr. Eser Çaktı ………………………………

Assoc. Prof. Kutay Orakçal …………………………..

DATE OF APPROVAL: 04.12.2014

ACKNOWLEDGEMENTS

I would first like to thank Prof. Dr. Erdal Şafak for his enlightening guidance and inspiring instructions in the development and completion of this study. I would like to express my sincere gratitude for his endless support and patience, and encouragement for my future career. It has been a great pleasure for me to be one of his students and work with such a great mentor.

Also, I would like to thank Prof. Dr. Eser Çaktı and Assoc. Prof. Kutay Orakçal for their time, attention and valuable comments.

I would like to thank faculty members, Assoc. Prof. Kemal Beyen, Assoc. Prof. Seval Pınarbaşı Çuhadaroğlu and Assoc. Prof. Şevket Özden, in the Civil Engineering department at Kocaeli University for their encouragement to pursue my masters after undergraduate.

I am grateful to all faculty members in the Earthquake Engineering Department for their support and contributions, especially Prof. Dr. Nuray Aydınoğlu and Prof Dr. Mustafa Erdik for their guidance during my studies.

I would like to thank all my friends and colleagues in the Earthquake Engineering Department, especially Okan İlhan and Caner Gülenç for our discussions about topics related to structural dynamics and Matlab. I appreciate Dr. Eren Vuran and Dr. H. Cem Yenidoğan's valuable support during my studies. I would also thank Dr. Yavuz Kaya for his enlightening contributions.

Last but not least, I would like to thank my parents, Selim Kocakaplan and Songül Kocakaplan for their unconditional love and understanding. My dear twin brother, Serkan Kocakaplan, I am grateful for all your love, support and sharing difficult times.

ABSTRACT

A METHOD TO CALIBRATE ANALYTICAL MODELS OF MULTI-STORY BUILDINGS FROM EARTHQUAKE RECORDS

For multi-story buildings, the standard approach to develop analytical models from earthquake records is to match the modal characteristics (*i.e.*, modal frequencies, damping ratios and mode shapes) of the model with those identified from the data. Typically, the response of the building is recorded in the basement, roof and a few intermediate floors. When the number of the instrumented floors is less than the total number of floors, an analytical model cannot be constructed uniquely. In other words, more than one model can match the recorded response.

This study presents a new method based on the transfer matrix formulation of the response. The method requires that vibration time histories are known at every floor. Since they are typically not recorded at every floor, we first present a methodology to estimate vibration time histories at non-instrumented floors from those of the instrumented floors. We assume that, at each modal frequency, the mode shape of a multi-story building can be approximated as a linear combination of the corresponding mode shapes of a shear beam and a bending beam. We determine the combination factors by using the least-squares approximation to the mode shapes identified from the records. The accuracy of the methodology is tested by using recorded motions from two buildings that have instruments at every floor. Assuming that only a few floors had instruments, the vibration time histories at other floors are calculated and compared with the recorded time histories. The results of the methodology are also compared with those from other approximation techniques, such as linear or cubic interpolations, and found to be much superior.

Once the vibration time histories are known at every floor, we present a new approach to calibrate analytical models of multi-story buildings based on the transfer matrix formulation of the response. The methodology utilizes top-to-bottom spectral-ratios at each

story and shows that these spectral ratios are not influenced by any structural changes in the stories below. Thus, starting from the top story, the stiffnesses of each story can be determined uniquely by matching the dominant frequencies of the spectral ratios, assuming that the mass of each floor is known or estimated. A numerical example is presented to confirm the validity of the approach.

The study proves that the story stiffnesses of a multi-story building can be determined uniquely by using vibration records taken from only a few floors.

ÖZET

ÇOK KATLI BİNALARIN ANALİTİK MODELLERİNİN DEPREM KAYITLARI KULLANILARAK KALİBRASYONU İÇİN BİR YÖNTEM

Çok katlı binaların analitik modellerinin deprem kayıtlarından geliştirilmesi için kullanılan standart yaklaşım, modelin modal karakteristiklerinin (örneğin, modal frekans, sönüm oranı ve mod şekilleri) kayıttan tanımlanmış olan modal karakteristikleriyle eşleştirilmesidir. Binaların tepkisi, tipik olarak bodrum katı, çatı ve bir kaç ara katta kayıt edilmektedir. Enstrümante edilmiş kat sayısının, toplam kat sayısından az olduğu durumlarda, analitik modellerin kalibrasyonu ilgili binanın analitik modeline özgün olmamaktadır. Diğer bir değişle, birden fazla analitik model kayıt edilmiş bina tepkisiyle eşleşebilir.

Bu çalışma, tepkinin transfer matrisi formülasyonunu kullanarak yeni bir yöntem sunmaktadır. Bu metotda, titreşimin zaman tanım alanındaki kayıtlarının her katta bilinmesi gerekmektedir. Ancak, kayıtlar genelde her katta alınmadığı için, öncelikle, enstrümante edilmemiş katlardaki titreşim kayıtlarının, enstrümante edilmiş katlardaki kayıtlardan hesaplanabilmesi için bir yöntem sunulmuştur. Bu yöntemde, çok katlı yapıların, her bir modal frekanstaki mod şekillerinin, kesme ve eğilme kirişi mod şekillerinin doğrusal bir kombinasyonu olarak elde edilebileceği varsayılmıştır. Kombinasyon çarpanları, kayıtlardan belirlenen mod şekillerine en küçük kareler yaklaşımı kullanılarak belirlenmiştir. Yöntemin doğruluğu, tüm katları enstrümante edilmiş olan iki yapı kullanılarak test edilmiştir. Sadece birkaç katta enstrüman olduğu varsayılarak, diğer katların titreşim kayıtları hesaplanmış ve ölçülen titreşim kayıtlarıyla karşılaştırılmıştır. Bu çalışmada geliştirilen yöntem, kullanılan diğer yaklaşık hesap yöntemleri (örneğin, doğrusal ve kübik interpolasyon) ile de karşılaştırılmış, ve sunulan yöntem ile daha iyi sonuçlar elde edildiği gösterilmiştir.

Her kattaki titreşimlerin zaman tanım alanındaki değerleri elde edildikten sonra, analitik modellerin kalibrasyonu için, tepkinin transfer matrisi formülüne dayalı yeni bir yöntem sunulmuştur. Bu yöntemle, her katın üst ve alt döşemelerindeki kayıtlarının spektral oranlarının, sadece o ve üstündeki katların yapısal karakteristiklerine bağlı olduğu, ve bu spektral oranların alt katta oluşacak olan hiç bir yapısal değişimden etkilenmediği gösterilmiştir. Bu nedenle, en üst kattan başlanılarak, birbirini izleyen katlar arasındaki spectral oranların hakim frekansları belirlenip, katlardaki kütle değerlerinin de bilindiği veya hesaplandığı varsayılarak, her bir katın hakim frekansına karşı gelen rijitliği bağımsız bir şekilde tayin edilebilir. Bu yaklaşımın geçerliliği örneklerle doğrulanmıştır.

Bu çalışma, çok katlı binalarda sadece bir kaç kattan elde edilmiş titreşim kayıtlarını kullanarak, her katın rijitlik değerlerinin bağımsız olarak belirlenebileceğini kanıtlamaktadır.

TABLE OF CONTENTS

LIST OF FIGURES

LIST OF TABLES

LIST OF SYMBOLS/ABBREVIATIONS

Caltech	California Institute of Technology
C1	Sensor configuration one
C2	Sensor configuration two
E	Young's modulus of elasticity
E-W	East-west
FAS	Fourier Amplitude Spectra
F_i	i^{th} floor internal force
G	Shear modulus
h	The height of the shear beam
I	The moment of inertia
L	The height of the bending beam
k_i	i^{th} floor stiffness
m	Mass per unit length
M	Moment magnitude
m_i	i^{th} floor mass
n	Mode number
N-S	North-south
SFAS	Smoothed Fourier amplitude spectra
t	Time
UCLA	University of California at Los Angeles
ω	Circular frequency
ω_n	n^{th} natural circular frequency
x_i	i^{th} floor total displacement
$\ddot{x}_g$	Base excitation
y_i	i^{th} floor displacement relative to base
ρ	The density
ϕ_n	n^{th} mode shape
ξ	Damping ratio

1. INTRODUCTION

1.1. Objectives of the Study

The objective of the study is to introduce a new method to calibrate analytical models of multi-story buildings from their vibration records. The accuracy of calibrated analytical models is directly related to the proper identification of the dynamic properties of the structure from vibration records. In general, records are available at a limited number of floors. As a result, calibration of analytical models from a limited number of records can cause non-unique models. The method introduced here requires that the vibration time histories are known at every floor. Since this is not typically the case, we first develop a methodology to estimate the vibration time histories at the non-instrumented floors by using the recorded vibrations at the instrumented floors, assuming that the real mode shape is a linear combination of the mode shapes of a bending beam and a shear beam. We call this approach the Mode Shape Based Estimation (MSBE) method.

Once the vibration time histories are known at every floor, we then present a calibration approach based on the transfer matrix formulation of the response, and use top-to-bottom spectral ratios of the records at each story to identify story stiffnesses uniquely.

1.2. Justification for the Study

For multi-storey buildings, analytical models are commonly developed from earthquake records by matching the identified modal characteristics from the records (*i.e.*, modal frequencies, damping ratios, and mode shapes) with those of the model. However, as mentioned earlier, records in most cases are available only at a limited number of floors. Models cannot be calibrated uniquely if they are based on records from a limited number of floors. In other words, more than one model can match the recorded properties of the structure. Moreover, modal properties can be influenced by environmental factors, as well as soil-structure interaction. Doebling *et al*. (1996) and Clinton *et al*. (2006) give examples of the effects of environmental factors (namely, temperature and rain) on modal frequencies. Similarly, soil-structure interaction also alters (*i.e.*, reduces) the fundamental frequency (Jennings and Bielak, 1973; Şafak, 1995; Stewart and Fenves, 1998; Trifunac *et*

al., 2010). Ideally, we would like to calibrate our model based on the fixed-base properties of the structure. It would be much harder to calibrate it with soil-structure interaction because of the frequency dependence of soil behaviour. Furthermore, it was shown that the fundamental frequency is not very sensitive to the changes in the physical characteristics of the structure. Trifunac *et al.* (2010) have investigated a threshold change in the building fundamental frequency that is associated with structural damage and they concluded that a drop off 20–30% in the fundamental frequency of a building may not necessarily lead to damage. Similarly, Şafak (2005) has shown, by using a 10-story analytical model that for a 10% reduction in the fundamental frequency, more than 40% reduction in the story stiffness is required.

More accurate analytical models can be developed, if we knew the vibration time histories at every floor. The common way to estimate vibration time histories at non-instrumented floors is to interpolate the calculated displacement time histories over the height of the building by using various interpolation techniques, such as linear, cubic, spline, etc. However, as will be explained in detail at Section 2, the accuracy of the interpolation is strongly dependent on where the instruments are placed (Goel, 2008). The MSBE (Mode Shape Based Estimation) methodology proposed in this study overcomes the limitations of the interpolation approaches.

Once the motions of every floor are known, a methodology based on the transfer matrix formulation of the response is introduced to calibrate analytical models from the recorded response.

1.3. Organization of the Study

Chapters 2 and 3 provide literature reviews on the estimation of building motions at non-instrumented floors, and the development of analytical models from vibration records, respectively.

Chapter 4 presents the theoretical background and the application of MSBE method. Equations for the least-squares approximation of the mode shapes of a building as a linear combination of the mode shapes of a shear beam and a bending beam are developed. The

methodology introduced are tested by using earthquake records from two densely instrumented buildings, the Factor Building at UCLA Campus in Los Angeles and the Millikan Library at Caltech in Pasadena, both of which have sensors at every floor.

Chapter 5 presents the new approach to develop analytical models from vibration records by using transfer matrix formulation of the response. A ten-story building model is used to illustrate the new approach.

Chapter 6 presents the conclusions of the study.

2. LITERATURE REVIEW

2.1. Estimation of Motions at Non-Instrumented Floors

For estimation of building motions at non-instrumented floors, the commonly used technique is the interpolation between the instrumented floors over the height of the building. The cubic and linear polynomial interpolation approaches have been used in many studies (De la Llera and Chopra, 1997; Goel, 2005, 2007; Skolnik *et al*., 2006, Naeim *et al*., 2006).

For the performance evaluations of 17 instrumented buildings after the January 17, 1994 Northridge Earthquake, Naeim (1997) has used a cubic spline interpolation, which results in smooth change between recorded data points, assuming that the recorded points are the knots of the cubic spline. He noted that cubic-spline interpolation is not suitable for base-isolated buildings. In Naeim *et al*. (2004), both cubic-spline and linear interpolations are used to predict the displacement response at each floor. The authors recommend that linear interpolation may be used for sub-basement levels of a tall building, but it should be combined with cubic interpolation for the floors above. The combination of cubic-linear interpolation procedure is also recommended for base-isolated buildings.

Limongelli (2003) proposed a criterion for the optimal location of sensors for structural health monitoring. The criterion relies on the reconstruction of seismic response, where no sensors are available. It is assumed that the recorded floors are the knots of cubic splines. An error function has been defined to measure the effectiveness of the cubic spline method. Optimal sensor locations are determined as those corresponding to the minimum value of the global error.

Goel (2008) discussed the accuracy of cubic polynomial interpolation approach in buildings with significant stiffness discontinuities. Using computer models, response time histories are calculated for selected buildings to simulate the motions at each floor. A limited number of simulated motions are used to test the accuracy of the cubic polynomial

interpolation. The results showed that the cubic interpolation is accurate if the building is instrumented at regular intervals over its height, and additional instruments are located in the building where stiffness changes significantly. Two reinforced-concrete buildings have been analysed to investigate the procedure. The results showed clearly that the accuracy of the method depends on the location of instrumented floors.

2.2. Developing Analytical Models from Vibration Records

A large number of studies have been conducted for the identification of the dynamic properties of structures from their vibration records. Consequently, different approaches and methodologies have been introduced to calibrate analytical models from the records. Beck and Katafygiotis (1998) suggested a model updating procedure, which is based on the coherency of the response of a finite-element model with the recorded response. Rahmani and Todorovska (2014) constructed analytical models based on the recorded wave propagation characteristics of the building.

Development of analytical models has been included in several review papers on SHM- Structural Health Monitoring (*e.g.*, Mottershead and Friswell, 1993). Chang *et al.* (2003) presented a review, which focused on the global health monitoring methods and the inaccuracies in the results. The paper states that the dynamic characteristics of structures may change due to environmental factors, such as temperature, moisture, and other environmental factors, and also some damage may not affect the natural frequencies. Another category of methods, known as Matrix Update Method, relies on updating the mass, damping and stiffness matrices of the model optimally to match the measured data. However, result of this optimization is not unique. Another review paper by Shon *et al.* (2004) covers the studies between 1996 and 2001. The authors point out that constructed analytical models are often uncertain and not fully validated with experimental data. Carden and Fanning (2004) provided a review that included various algorithms in time, frequency and modal domains. The authors explained that, in case of limited amount of measured data coupled with a large number of individual parameters, model updating methods can result in non-unique solutions.

Kunnath *et al.* (2004) is carried out an evaluation of the four analytical methods recommended in *FEMA-356* for the estimation of seismic demands on two instrumented steel buildings. A 6-story building with no visible signs of damage was calibrated by using records from three earthquakes. The calibration first aimed to match the fundamental period identified from the Northridge Earthquake. The model was further calibrated by using the data from the Whittier-Narrows Earthquake, which required an increase in the stiffness. The results showed that Whittier-Narrows calibrated model is too stiff to re-produce the Northridge response, and Northridge calibrated model is too soft to re-produce Whittier-Narrows response. The main reason for the difference is the participation of non-structural members in the latter one. They concluded that calibrating structural models to observed response is sensitive to the assumptions in modelling the mass and the stiffness, and indirectly, to the intensity of ground motion.

Goel (2005) has investigated the FEMA-356 Nonlinear Static Procedure (NSP) and Modal Pushover Analysis (MPA) procedure by using the recorded motions of four buildings that were damaged during the 1994 Northridge Earthquake. The author pointed out that recorded motions of buildings, especially those deformed into the inelastic range, provide a unique opportunity to evaluate calibration procedures. The analytical models are calibrated by matching the fundamental period of the model and the elastic period obtained from the system identification. The accelerations recorded at the base are used as the input motion to the model in order compute the time histories of floor displacements and story drifts.

3. ESTIMATION OF MOTIONS AT NON-INSTRUMENTED FLOORS

Multi-story buildings deform in shear and bending. In short buildings and buildings with no shear walls; the response is dominated by shear-type deformations, whereas in tall buildings and buildings with shear walls, the response is dominated by bending-type deformations. Therefore, we can reasonably assume that the response of a typical multi-story building is a combination of shear and bending-type deformations.

Several researchers have considered only shear-type deformations for the equivalent model of buildings (*e.g.*, Westergaard 1933, Jennings and Newmark, 1960, Iwan 1997). Some researchers used Bernoulli-Euler beams to model flexural-type deformations (*e.g.*, Foutch and Jennings, 1978). Miranda (1999) and Miranda and Akkar (2006) have used an equivalent continuum model, which is a combination of flexural and shear cantilever beams, to estimate the maximum roof displacements and inter-story drifts of buildings responding mainly in the first mode. Figure 3.1, adopted from Miranda (1999), shows schematically the bending and shear deformations, and the total deformation.
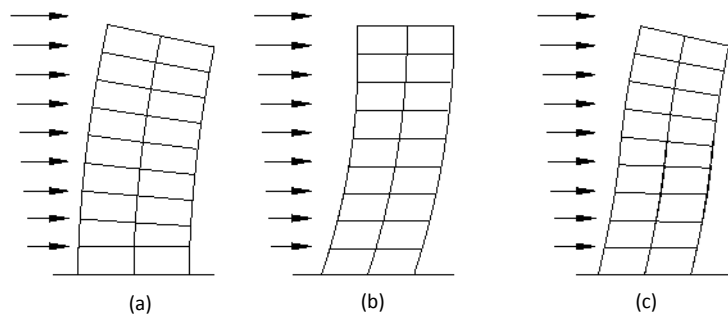
Figure 3.1. Deformations of buildings: (a) bending, (b) shear, and (c) total.

Based on the arguments above, we propose that the behaviour of a multi-story building at each mode (*i.e.*, the mode shape) can be approximated as a linear combination of the corresponding mode shapes of a shear beam and a bending beam.

3.1. Mode Shapes of a Shear Beam

The natural frequencies and the corresponding mode shapes of shear beam can be identified through the solution of the following differential equation (Chapter 67, Jennings, 2003):

$$\frac{\partial^2 u}{\partial t^2} - \frac{G}{\rho}\frac{\partial^2 u}{\partial x^2} = f(x,t) \tag{3.1}$$

here, G is the shear modulus and ρ is the density. Boundary conditions are:

$$\text{At the clamped end: } u = 0; \quad \text{at the free end: } \partial u/\partial x = 0 \tag{3.2}$$

with these boundary conditions, the equations for the natural frequencies and the mode shapes are found to be (Chapter 67, Jennings, 2003):

$$\omega_n = \sqrt{\frac{G}{\rho}} \cdot \frac{(2n-1)\pi}{2h}, \quad n = 1,2,3 \dots \tag{3.3}$$

$$\phi_n(x) = sin\frac{(2n-1)\pi \cdot x}{2h}, \quad n = 1,2,3 \dots \tag{3.4}$$

where h is the height of the beam.

3.2. Mode Shapes of a Bending Beam

Deformations of a bending beam occur as extensions on the convex side (due to lengthening) and compressions on the concave side (due to shortening). The natural frequencies and the corresponding mode shapes of a bending beam can be obtained by solving the following differential equation (Chopra, 2007):

$$m\frac{\partial^2 u(x,t)}{\partial t^2} + EI\frac{\partial^4 u(x,t)}{\partial x^4} = f(x,t) \tag{3.5}$$

Here, $u(x,t)$ is the transverse deflections of the beam under the external dynamic forces $f(x,t)$, x is span wise coordinate, m is mass per unit length, EI is the flexural rigidity of the beam, where E is the Young's Modulus of elasticity and I is the moment of inertia. The general solution for the spatial function is:

$$\phi(x) = C_1 sin\beta x + C_2 cos\beta x + C_3 sinh\beta x + C_4 cosh\beta x \qquad (3.6)$$

where

$$\beta^4 = \frac{\omega^2 m}{EI} \qquad (3.7)$$

The four unknown constants, C_1, C_2, C_3 and C_4, are determined from the following four boundary conditions:

$$\text{At the clamped end } u = 0 \quad \text{and} \quad \frac{\partial u}{\partial x} = 0 \qquad (3.8a)$$

$$\text{At the free end:} \quad \frac{\partial^2 u}{\partial x^2} = 0 \quad \text{and} \quad \frac{\partial^3 u}{\partial x^3} = 0 \qquad (3.8b)$$

Based on these, the modal equations for a cantilever bending beam becomes:

$$1 + cos\beta L \, cosh\beta L = 0 \qquad (3.9)$$

By solving numerically, we find the following for the first four modes:

$$\beta_n L = 1.8751, 4.6941, 7.8548 \text{ and } 10.996 \qquad (3.10)$$

For $n>4$, $\beta_n L \cong (2n - 1)\pi/2$. The corresponding natural frequencies and the mode shapes for a bending beam are:

$$\omega_n^2 = \frac{\beta_n{}^4 (EI)}{m} \qquad (3.11)$$

$$\phi_n(x) = C_n\left[cosh\beta_n x - cos\beta_n x - \frac{cos\beta L + cosh\beta L}{sin\beta L + sinh\beta L}(sinh\beta x - sin\beta x)\right] \qquad (3.12)$$

The comparisons of the first six modes of a shear beam and a bending beam are shown in Figure 3.2. The mode shapes are normalized by the amplitude of top floor.
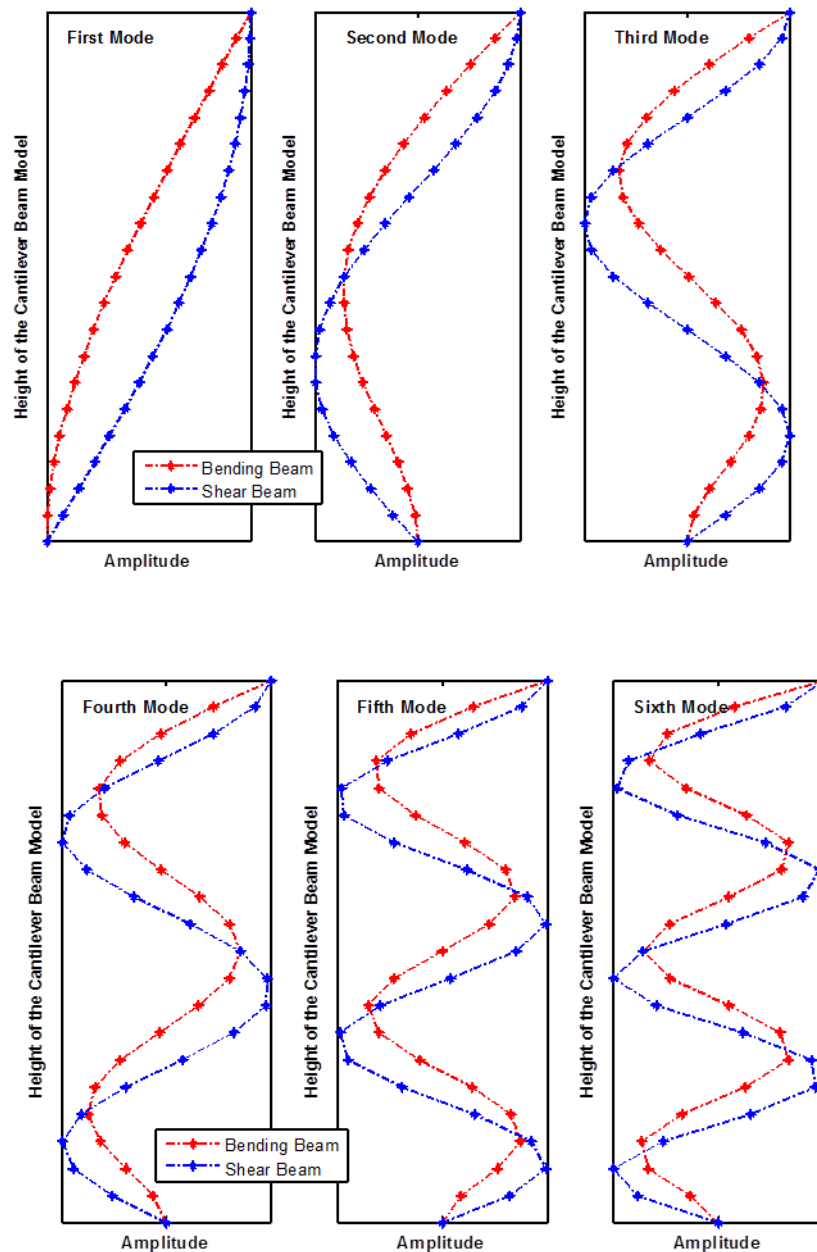
Figure 3.2. The comparisons of first six modes of the shear beam and the bending beam.

It can be observed from Figure 3.2 that the slopes of mode shapes are different and the peaks occur at different heights. More detail on the modal characteristics of shear and bending beams can be found elsewhere (*e.g.*, Chopra, 2007; Chapter 67, Jennings, 2003).

3.3. Least-Squares Approximation of Mode Shapes

For an N-story linearly elastic multi-story building subjected to earthquake loads, the displacements relative to ground can be calculated by the superposition of modal displacements, as

$$u_{j,k}(t) = \Gamma_j \cdot \phi_{j,k} \cdot q_j(t) \tag{3.13a}$$

$$u_k(t) = \sum_{j=1}^{N} \Gamma_j \cdot \phi_{j,k} \cdot q_j(t) \tag{3.13b}$$

where:

$u_{j,k}(t)$: time variation of the jth mode relative displacement at k[th] floor;

$u_k(t)$: time variation of the total relative displacement at k[th] floor;

Γ_j : modal participation factor for the jth mode;

$\phi_{j,k}$: amplitude of the jth mode at k[th] floor; and

$q_j(t)$: time-variation of the displacement of jth mode.

$q_j(t)$ is calculated from the following modal equation:

$$\ddot{q}_j(t) + 2\zeta_j \omega_j \dot{q}_j(t) + \omega_j^2 q(t) = -\ddot{u}_g(t) \tag{3.14}$$

where ζ_j and ω_j are damping ratio and frequency, respectively, for the jth mode; $\ddot{u}_g(t)$ is the time variation of ground accelerations. Denoting the jth modal displacement as $D_j(t) = \Gamma_j \cdot q_j(t)$, the Equations 3.13a and 3.13b will lead to,

$$u_{j,k}(t) = \phi_{j,k} \cdot D_j(t) \tag{3.15a}$$

$$u_k(t) = \sum_{j=1}^{N} \phi_{j,k} \cdot D_k(t) \tag{3.15b}$$

The MSBE (Mode Shape Based Estimation) method proposed in this study assumes that the mode shape of a building can be approximated as the linear combination of the corresponding mode shapes of a shear beam and a bending beam as shown below:

$$\phi_{j,k} = C_{s,j} \cdot \phi_{s,j,k} + C_{b,j} \cdot \phi_{b,j,k} \tag{3.16}$$

where $\phi_{s,j,k}$ and $\phi_{b,j,k}$ are the amplitudes of the jth mode shapes of a shear beam and a bending beam, respectively, at k^{th} floor; $\phi_{j,k}$ is the amplitude of the jth mode shape of the multi-storey building at k^{th} floor; $C_{s,j}$ and $C_{b,j}$ are the unknown weighting factors (*i.e.*, shear and bending contributions) for the jth mode. For each mode and each time instant, the error in the approximation can be expressed as the square sum of the differences over the instrumented floors between the recorded modal displacements, $y_{j,k}(t)$, and the calculated modal displacements, $u_{j,k}(t)$:

$$\varepsilon_j(t) = \sum_{i=1}^{NIF} \left[y_{j,k}(t) - u_{j,k}(t) \right]^2 \tag{3.17}$$

where $\varepsilon_j(t)$ is the error function for the jth mode; *NIF* is the number of instrumented floors.

In order to calculate the recorded modal displacements, $y_{j,k}(t)$, the recorded accelerations at each instrumented floors are first band-pass filtered around each modal frequency and then double integrated. The summation in the error function (Equation 3.17) is over the instrumented floors. The coefficients $C_{s,j}$ and $C_{b,j}$ can be estimated by minimizing the error function as:

$$\frac{\partial \varepsilon_j}{\partial C_{s,j}} = 0, \qquad \frac{\partial \varepsilon_j}{\partial C_{b,j}} = 0 \tag{3.18}$$

which leads to,

$$\frac{\partial \varepsilon_j}{\partial C_{s,j}} = \sum_{i=1}^{NIF} -2\phi_{s,j,k}\, y_{j,k}(t)D_j(t) + 2C_{s,j}\phi_{s,j,k}^2 D_j^2(t) + 2C_{b,j}\phi_{s,j,k}\phi_{b,j,k}D_j^2(t)$$

$$\frac{\partial \varepsilon_j}{\partial C_{b,j}} = \sum_{i=1}^{NIF} -2\phi_{b,j,k}\, y_{j,k}(t)D_j(t) + 2C_{b,j}\phi_{b,j,k}^2 D_j^2(t) + 2C_{s,j}\phi_{s,j,k}\phi_{b,j,k}D_j^2(t)$$

(3.19)

$$\begin{bmatrix} \sum_{i=1}^{NIF}\phi_{s,j,k}^2 & \sum_{i=1}^{NIF}\phi_{s,j,k}\cdot\phi_{b,j,k} \\ \sum_{i=1}^{NIF}\phi_{s,j,k}\cdot\phi_{b,j,k} & \sum_{i=1}^{NIF}\phi_{b,j,k}^2 \end{bmatrix} \cdot \begin{pmatrix} C_{s,j}\cdot D_j(t) \\ C_{b,j}\cdot D_j(t) \end{pmatrix} = \begin{bmatrix} \sum_{i=1}^{NIF}\phi_{s,j,k}\cdot y_{j,k}(t) \\ \sum_{i=1}^{NIF}\phi_{b,j,k}\cdot y_{j,k}(t) \end{bmatrix}$$

(3.20)

Equation 3.20 can be simplified for j^{th} mode as,

$$M_j \cdot W_j(t) = Y_j(t)$$ (3.21)

where M_j is a constant time-invariant matrix, and its elements are a linear function of the jth mode shapes of a bending and a shear beam only; $W_j(t)$ is the contributions from the shear beam and the bending beam into the jth modal displacement at time t; and $Y_j(t)$ is the input matrix containing recorded responses at the instrumented floors at time t. Equation 3.21 has to be satisfied at every time step, t. Note that the matrix M_j is time-independent and, therefore, needs to be calculated only once. However, the matrix $Y_j(t)$ is time-dependent and must be calculated at every time step, t.

Using Equations 3.15 and 3.21, j^{th} modal displacement at k^{th} floor, $u_{j,k}(t)$ can be calculated by multiplying $W_j(t)$ by $[\phi_{s,j,k} \quad \phi_{b,j,k}]$ as,

$$u_{j,k}(t) = [\phi_{s,j,k} \quad \phi_{b,j,k}] \cdot \begin{bmatrix} C_{s,j}\cdot D_j(t) \\ C_{b,j}\cdot D_j(t) \end{bmatrix}$$ (3.22)

The unknown weighting coefficient of $C_{s,j}$ and $C_{b,j}$ for a specific time instant, can be calculated as,

$$C_{s,j} = \frac{\left[\sum_{i=1}^{NIF} \phi_{s,j,k}{}^2\right]\left[\sum_{i=1}^{NIF} \phi_{s,j,k}\, y_{j,k}\right] - \left[\sum_{i=1}^{NIF} \phi_{b,j,k}\phi_{s,j,k}\right]\left[\sum_{i=1}^{NIF} \phi_{b,j,k}\, y_{j,k}\right]}{\left[\sum_{i=1}^{N} \phi_{s,j,k}{}^2\right]\left[\sum_{i=1}^{N} \phi_{b,j,k}{}^2\right] - \left[\sum_{i=1}^{NIF} \phi_{b,j,k}\phi_{s,j,k}\right]\left[\sum_{i=1}^{NIF} \phi_{s,j,k}\, \phi_{b,j,k}\right]}$$

(3.23)

$$C_{b,j} = \frac{\left[-\sum_{i=1}^{NIF} \phi_{s,j,k}\, \phi_{b,j,k}\right]\left[\sum_{i=1}^{NIF} \phi_{s,j,k}\, y_{j,k}\right] + \left[\sum_{i=1}^{NIF} \phi_{s,j,k}{}^2\right]\left[\sum_{i=1}^{NIF} \phi_{b,j,k}\, y_{j,k}\right]}{\left[\sum_{i=1}^{NIF} \phi_{s,j,k}{}^2\right]\left[\sum_{i=1}^{NIF} \phi_{b,j,k}{}^2\right] - \left[\sum_{i=1}^{NIF} \phi_{b,j,k}\phi_{s,j,k}\right]\left[\sum_{i=1}^{NIF} \phi_{s,j,k}\, \phi_{b,j,k}\right]}$$

The kth floor displacement then becomes:

$$u_k(t) = \sum_{j=1}^{N} u_{j,k}(t)$$

(3.24)

where *NIM* is the number of identified modes.

3.4. Confirmation of the MSBE method

The accuracy of the MSBE method is tested by utilizing the earthquake records from the UCLA's Factor Building in Los Angeles, California and from the Caltech's Millikan Library in Pasadena, California.

Both buildings are densely instrumented with accelerometers at every floor. To test the methodology, it is assumed that the accelerations were available only from a few floors. The accelerations from the remaining floors are estimated by using the MSBE method, and then compared with the recorded ones. The results are also compared with those calculated by using linear and cubic polynomial interpolation methods.

3.4.1. The UCLA Factor Building

The UCLA's Doris and Louis Factor building, a 17-story moment resisting steel frame, is one of the most densely instrumented buildings in the world. The building is the

tallest structure on the campus with standing approximately 74.52 meters from its base. After 1994 Northridge, California Earthquake, the Factor Building was instrumented by the U.S. Geological Survey with 72-channel accelerometer operating in real time. Since then, large amount of earthquake and ambient vibration data have been collected. More information about the structure and the instrumentation can be found in Kohler *et al*. (2005). Figure 3.3 shows a picture of the building, taken from the north-east side, and sensor layout.
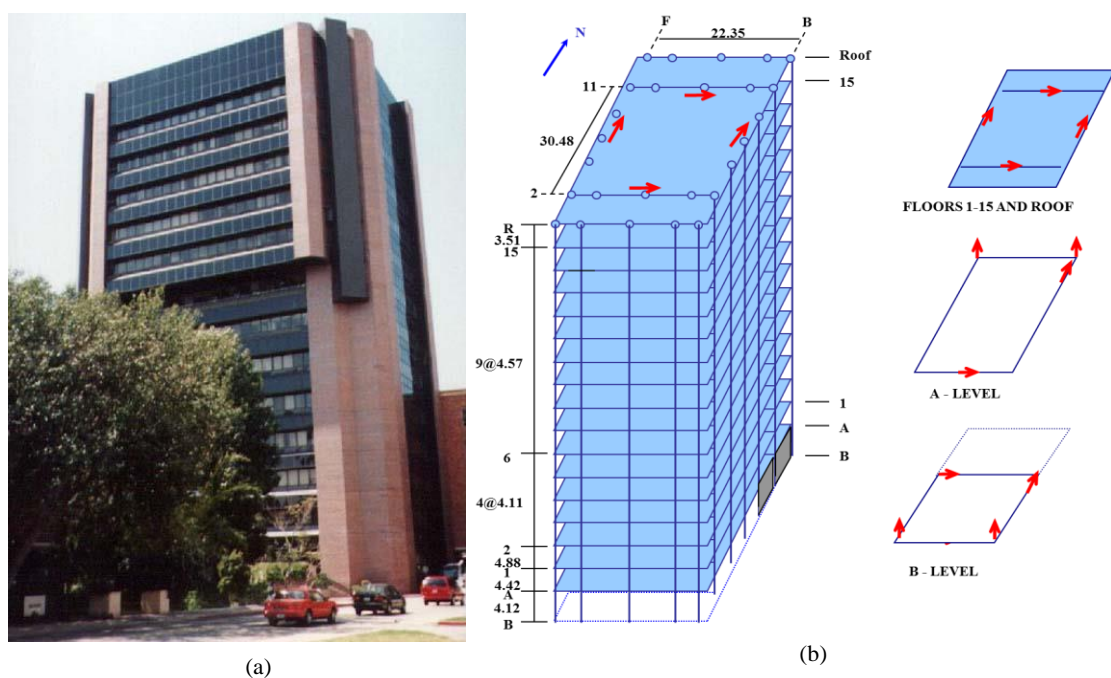
Figure 3.3. (a) Northeast side of The UCLA Factor Building (b) Sensor layout of the structure and arrows show the polarities of sensors on each floor (Kohler *et al.,* 2005).

3.4.1.1. Selected Earthquake Data. To test the accuracy of the MSBE method on the Factor Building, we have used data from two earthquakes: M=6.0 Parkfield, California Earthquake of 28 September 2004 and M=4.8 Yorba Linda, California Earthquake of 3 September 2002. The epicentral distances of the earthquakes from the building were 262 km for the former and 64 km for the latter. The Yorba Linda Earthquake differs from the Parkfield Earthquake for having more energy in high frequencies, and consequently greater influence in higher modes of the building.
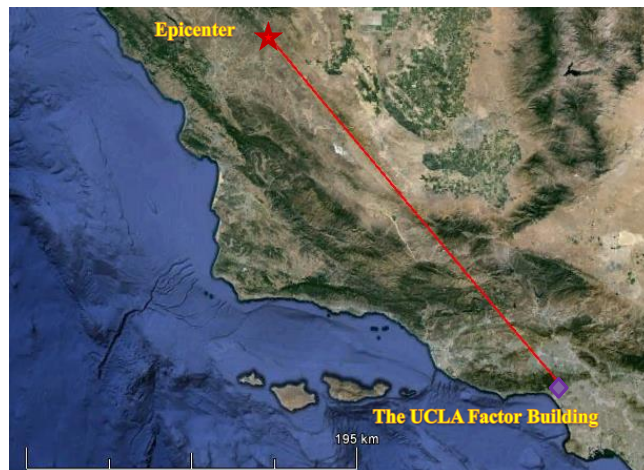
Figure 3.4. Map showing the location of Parkfield Earthquake and the Factor Building.

Figure 3.5. Map showing the location of Yorba Linda Earthquake and the Factor Building.

3.4.1.2. Identification of Modal Properties and Application of the MSBE Method. The accuracy of the method is demonstrated by using two different sensor configurations for each selected earthquake. The first configuration (C1) assumes that the sensors are located on the 1st and the 7th floors, and the roof, while in the second sensor configuration (C2) the sensors are located on the 1st and the 13th floors, and the roof.

Figure 3.6 shows the east-west and north-south components of the recorded accelerations at Factor Building from the Parkfield Earthquake.
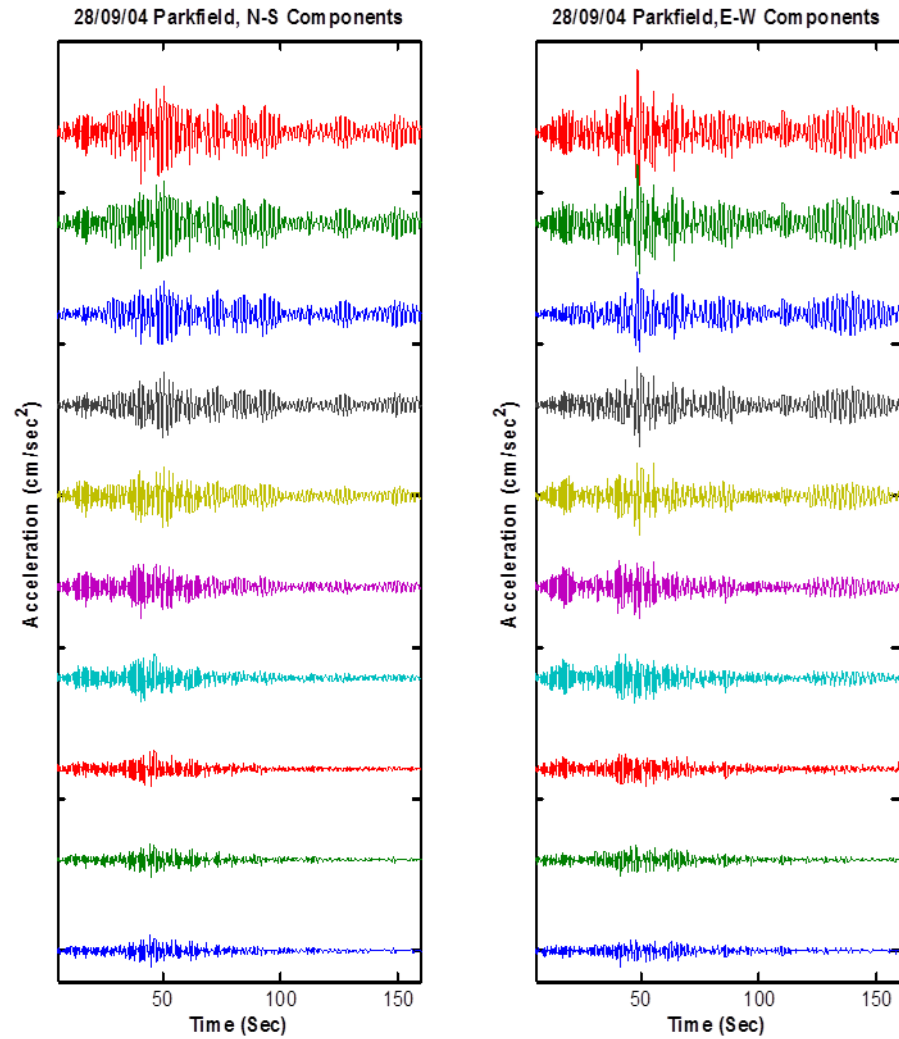
Figure 3.6. Recorded accelerations at Factor Building during the M=6.0 Parkfield Earthquake of 28 September 2004: (a) the north-south component of the accelerations recorded on the east side, and (b) the east-west components of the accelerations recorded on the south side.

Results of the MSBE approximation for the C1 and C2 sensor configurations will be shown by using the east-west components of the south-side sensors. The same tests have been performed by using the records from other sensors and component, and the results were found to be similar.

The first step in the application of MSBE method is to identify the modal frequencies from the records of instrumented floors. Modal frequencies of building-type structures can be identified by using simple spectral techniques given in Şafak and Çaktı (2014). Before the calculation of Fourier Amplitude Spectra (FAS), the records are band-pass filtered between 0.05-5.0 Hz, and a Hanning window is applied to reduce spectral leakage. The calculated FAS are then smoothed by using running triangular smoothing windows with optimum lengths. The optimum lengths of smoothing windows are determined as suggested in Şafak (1997). The Smoothed FAS (SFAS) are given in Figure 3.7 for the C1 sensor configuration and in Figure 3.8 for the C2 sensor configuration. The identified frequencies are given in Table 3.1. The values in the table are in good agreement with the values calculated by others (*e.g.*, Skolnik *et al*., 2006).

Table 3.1. Identified translational modal frequencies of the Factor Building.

Direction	First Horizontal Mode (Hz)	Second Horizontal Mode (Hz)	Third Horizontal Mode (Hz)
East-West	0.4-0.5	1.4-1.5	2.6-2.7
North-South	0.5-0.6	1.6-1.7	2.8-2.9
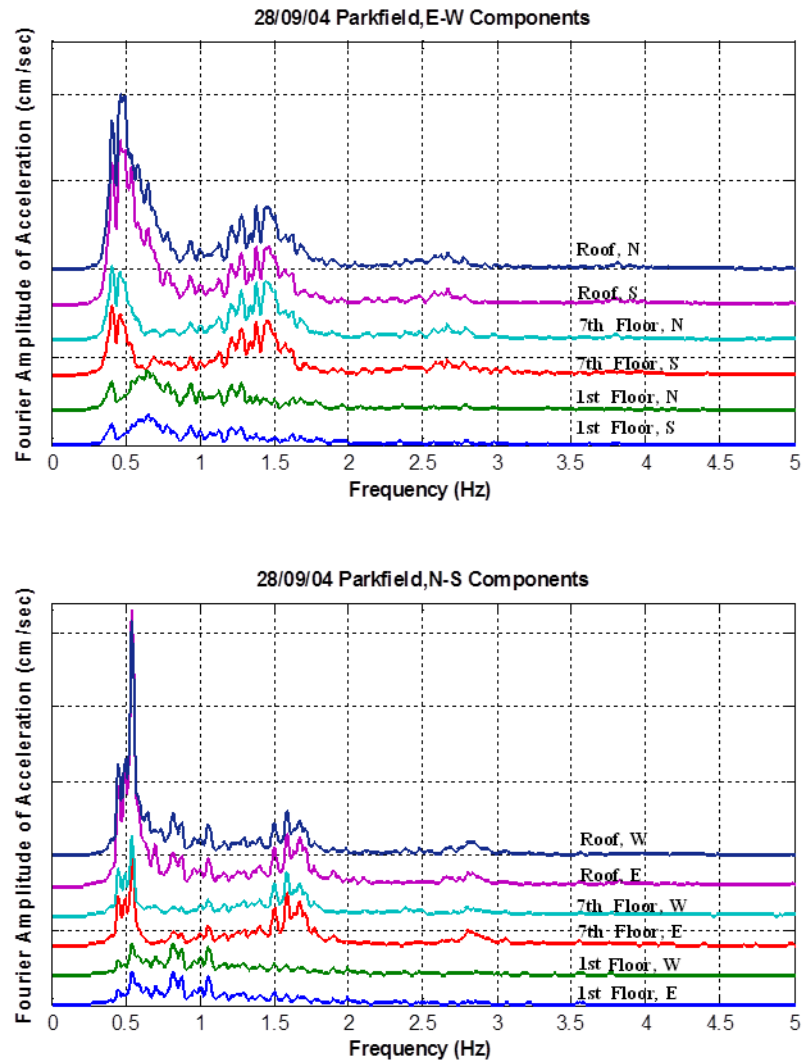
Figure 3.7. Smoothed Fourier Amplitude Spectrum of the Parkfield Earthquake records For C1 sensor configuration. (a) East-west direction records (b) North-south direction records.
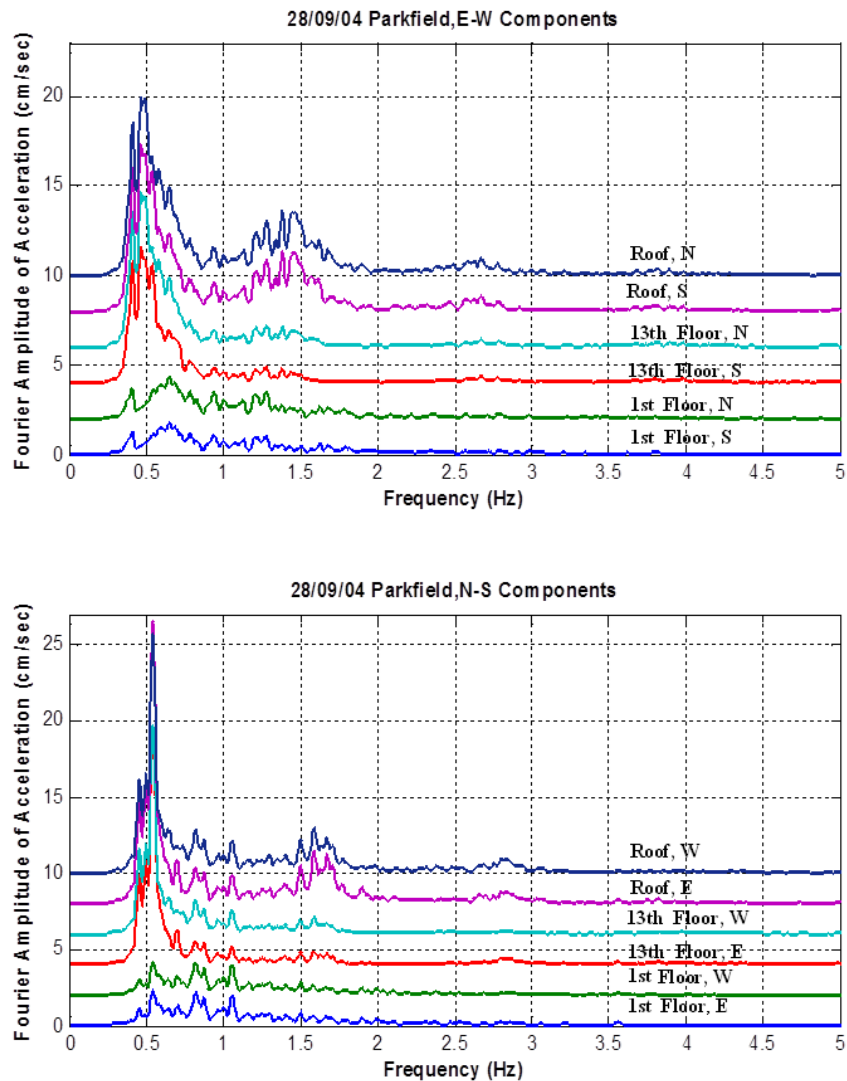
Figure 3.8. Smoothed Fourier Amplitude Spectrum of the Parkfield Earthquake, records for C2 sensor configuration. (a) East-west direction records (b) North-south direction records.

The recorded accelerations from the Parkfield Earthquake are first narrow band-pass filtered around the identified frequencies in Table 3.1. They are then double integrated to obtain modal displacements at corresponding floors. Dominant directions of each mode are determined by plotting roof configuration, assuming rigid floors. The plots show mainly uni-directional modes with not much torsion. Roof configurations for the fundamental modes in each direction are illustrated in Figure 3.9 for the consecutive three peaks (each colour represents the successive peaks).
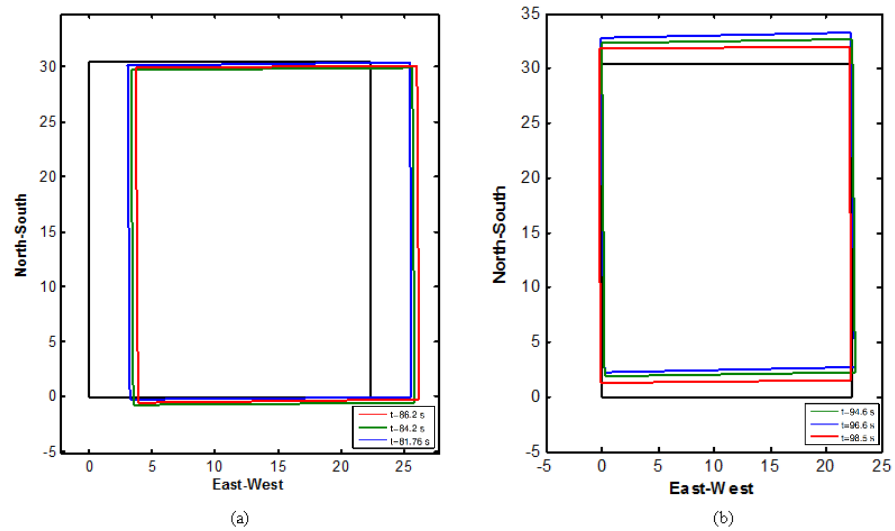
Figure 3.9. Roof displacements. (a) First east-west mode (b) First north-south mode.

For each mode, the modal displacements at the non-instrumented floors are estimated from the modal displacements at the instrumented floors by using the MSBE methodology discussed earlier. The time-history of the total displacement at a non-instrumented floor is calculated by adding the time histories of the modal displacements.

The comparison of recorded and MSBE (*i.e.*, least-squares) calculated modal displacements along the height (*i.e.*, the mode shapes) for the Parkfield Earthquake are shown in Figures 3.10 and 3.11 for the C1 and C2 sensors configurations, respectively. Also shown in the figures are the shapes that a linear or a cubic spline interpolation would give.
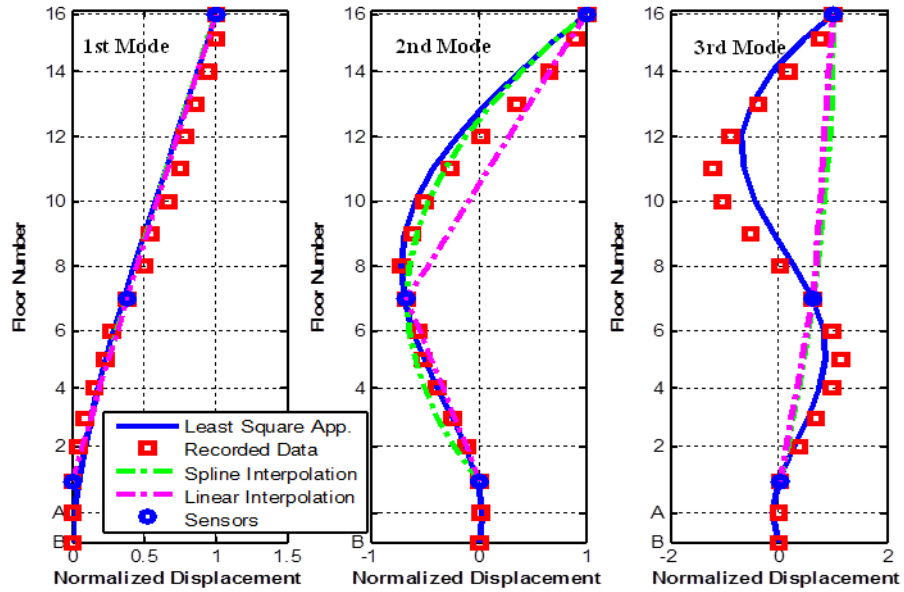
Figure 3.10. Mode shapes are normalized by the roof displacement. Blue lines represent the estimated mode shapes for the C1 sensor configuration while red squares are the actual mode shapes calculated by using the records from all floors. The dashed-green and dashed-pink lines demonstrate the spline and linear interpolations, respectively.
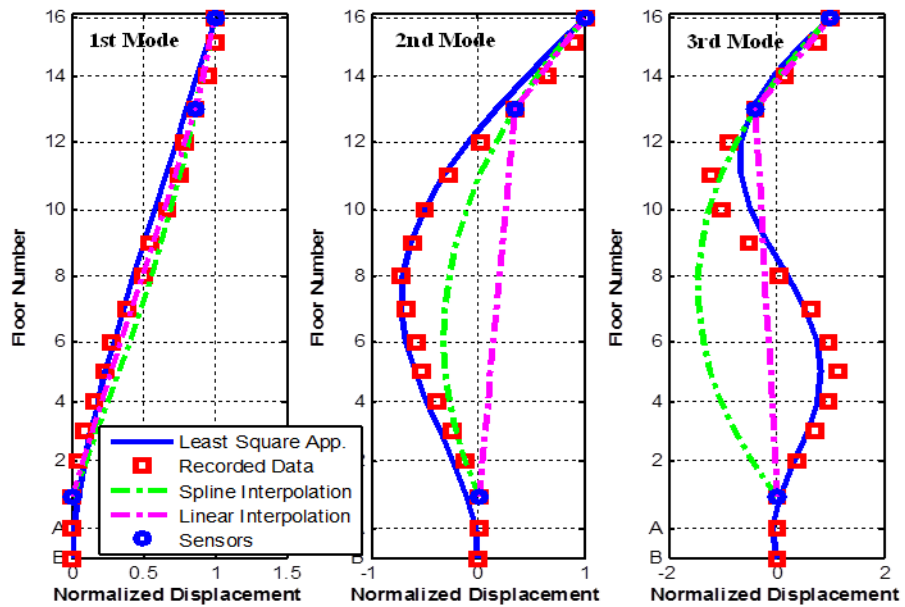
Figure 3.11. Mode shapes are normalized by the roof displacement. Blue lines represent the estimated mode shapes for the C2 sensor configuration while red squares are the actual mode shapes calculated by using the records from all floors. The dashed-green and dashed-pink lines demonstrate the spline and linear interpolations, respectively.

The modal displacements for the second mode indicate that second mode can be divided approximately into two linear segments around the 8th floor level. As the middle sensor moves to the upper or lower floors, estimation of the second mode for the linear interpolation method will decrease. It can be also inferred from the Figure 3.10 and Figure 3.11 that both cubic-spline and linear interpolation methods fail to give a good estimation for the third mode shape.

Figures 3.12 and 3.13 show, for the C1 configuration, the comparison of the recorded and predicted displacement-time histories by the three approximation techniques at the 4th and 10th floors, which were assumed to be non-instrumented. Figures 3.14 and 3.15 show the same for the C2 configuration. All three estimation techniques give a good estimate of the displacement-time histories at the 4th and 10th floors. The reason for this is that the first mode dominates the response, and all three methods give a very good approximation of the first mode shape. The matches were equally good for the other assumed to be non-instrumented floors. The accuracy of the linear or cubic-spline interpolation estimations get worse as the contribution from higher modes become significant. This will be shown below by using the records from the Yorba Linda Earthquake.
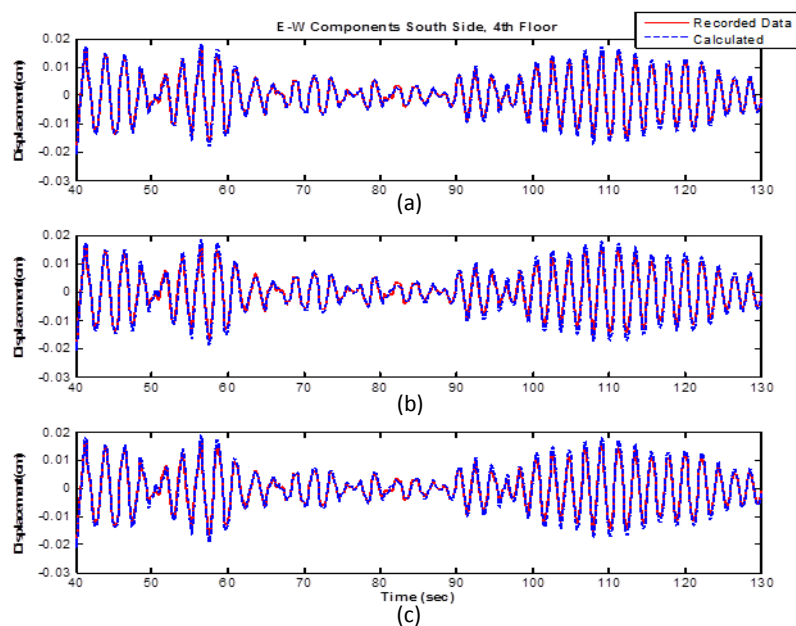
Figure 3.12. Comparison of recorded and estimated displacement time histories at the 4th floor for the C1 sensor configuration. (a) MSBE method (b) Linear interpolation (c) Cubic-spline interpolation.
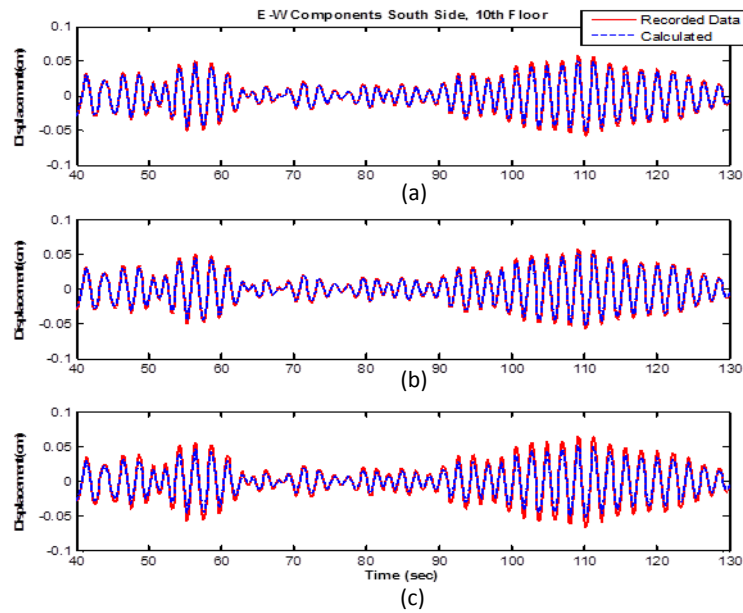
Figure 3.13. Comparison of recorded and estimated displacement time histories at the 10th floor for the C1 sensor configuration. (a) MSBE method (b) Linear interpolation (c) Cubic-spline interpolation.
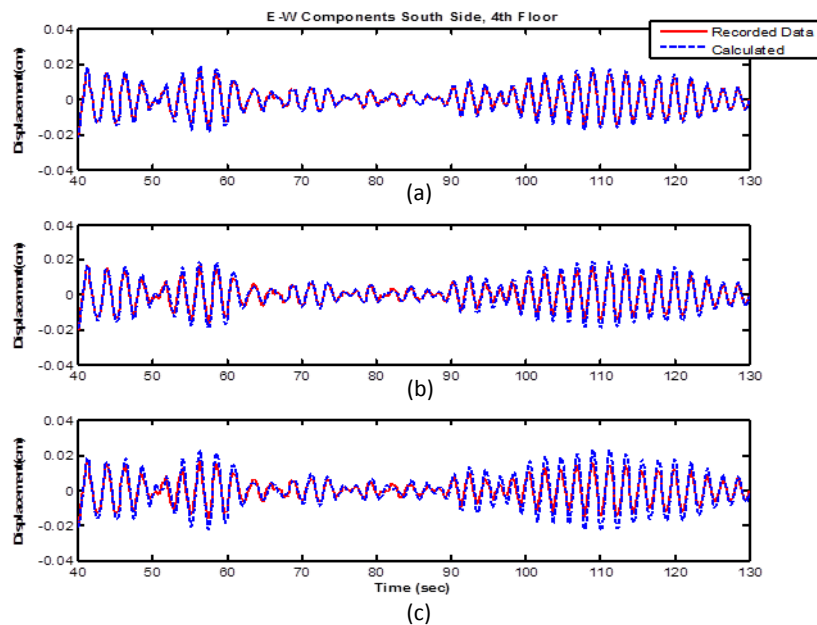
Figure 3.14. Comparison of recorded and estimated displacement time histories at the 4th floor for the C2 sensor configuration. (a) MSBE method (b) Linear interpolation (c) Cubic-spline interpolation.
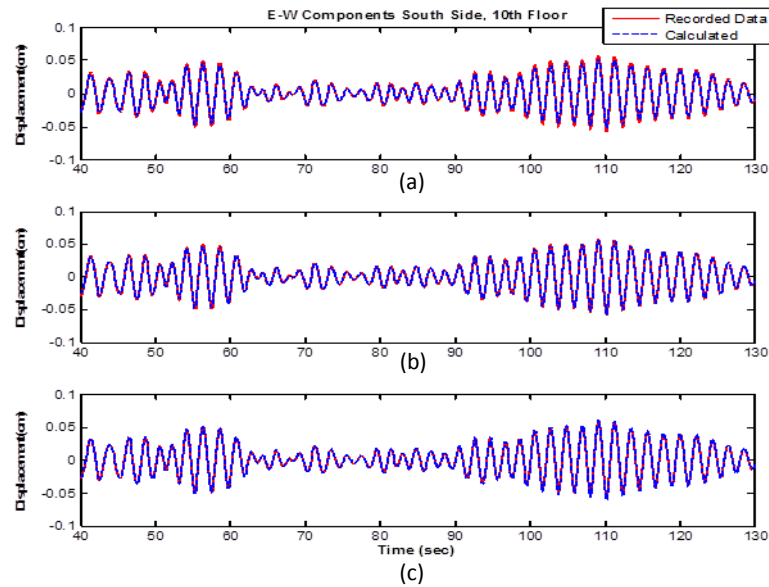
Figure 3.15. Comparison of recorded and estimated displacement time histories at the 10th floor for the C2 sensor configuration. (a) MSBE method (b) Linear interpolation (c) Cubic-spline interpolation.

The frequency content of the Yorba Linda Earthquake is richer in high frequencies, and therefore it has greater influence on the higher modes of the Factor Building.
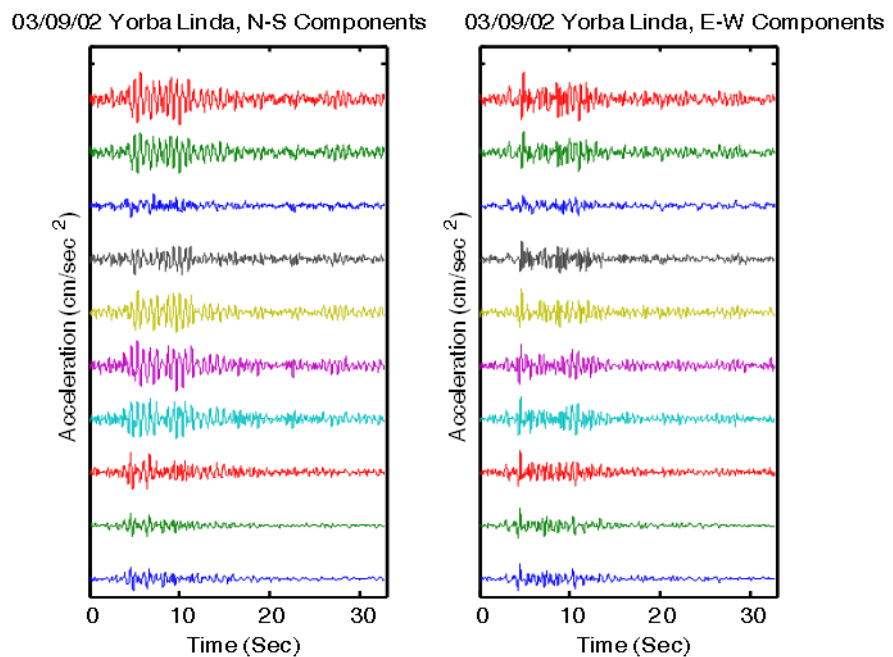
Figure 3.16. Acceleration time histories of the Factor Building after the Yorba Linda Earthquake of 3 September 2002.

Figure 3.16 shows the acceleration-time histories of the Yorba Linda Earthquake over the height of the building. Fourier amplitude spectrum of both C1 and C2 sensor configurations are calculated and plotted in Figure 3.17 and Figure 3.18, respectively. Modal frequencies identified are listed in Table 3.2.

Table 3.2. Identified translational modal frequencies of the Factor Building.

Direction	First Horizontal Mode (Hz)	Second Horizontal Mode (Hz)	Third Horizontal Mode (Hz)	Fourth Horizontal Mode (Hz)
East-West	0.4-0.6	1.4-1.6	2.6-2.8	3.9-4.1
North-South	0.5-0.7	1.65-1.92	2.8-3.2	-
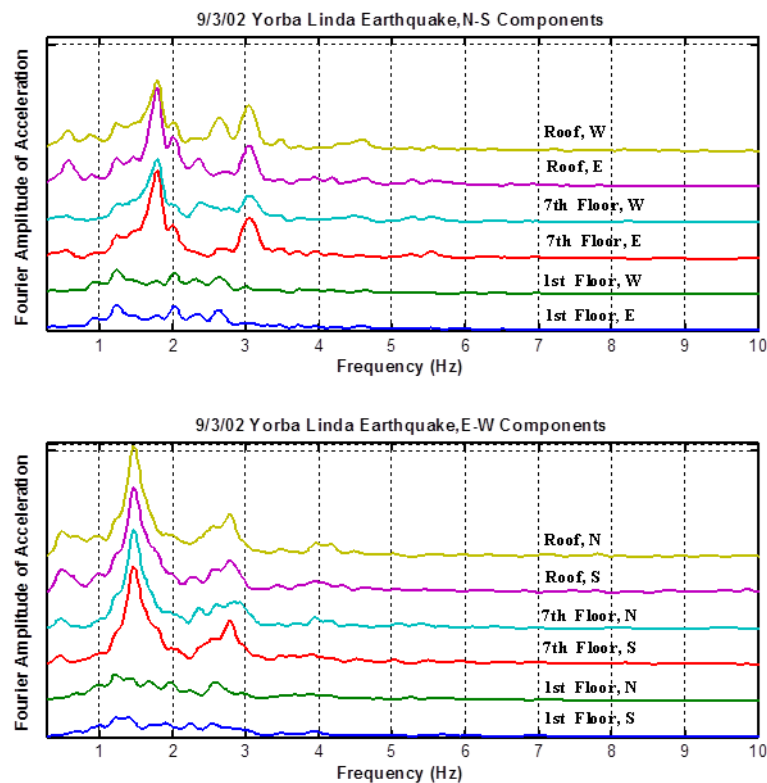
Figure 3.17. Smoothed Fourier Amplitude Spectrum of the Yorba Linda Earthquake records for C1 sensor configuration. (a) East-west direction records (b) North-south direction records.
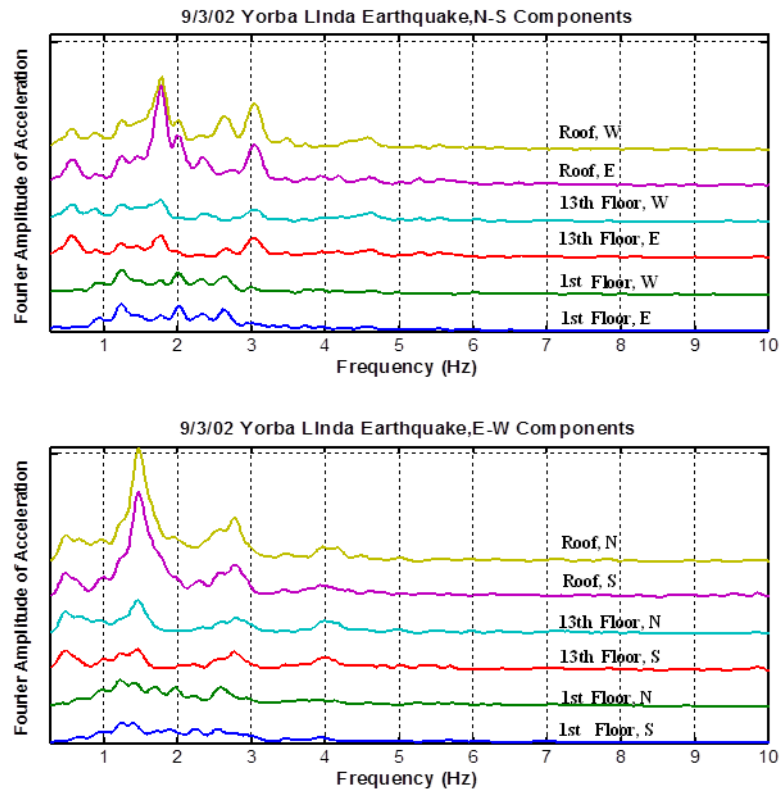
Figure 3.18. Smoothed Fourier Amplitude Spectrum of the Yorba Linda Earthquake records for C2 sensor configuration. (a) East-west direction records (b) North-south direction records.

Acceleration time histories are band-pass filtered around each identified modal frequency, listed in the table, and then double integrated to obtain corresponding modal displacement time histories. Directions of the modes are confirmed by examining the particle motions of the roof. Figures 3.19 and 3.20 show the first four-mode shapes of the Factor building that are calculated by using the MSBE method, as well as the linear and cubic interpolations approximations for comparison, for the C1 and C2 sensor configurations. Amplitudes of the mode shapes at each floor level correspond to the modal displacement at that floor. Mode shapes are plotted for the east-west components of the sensors on the south wall only.
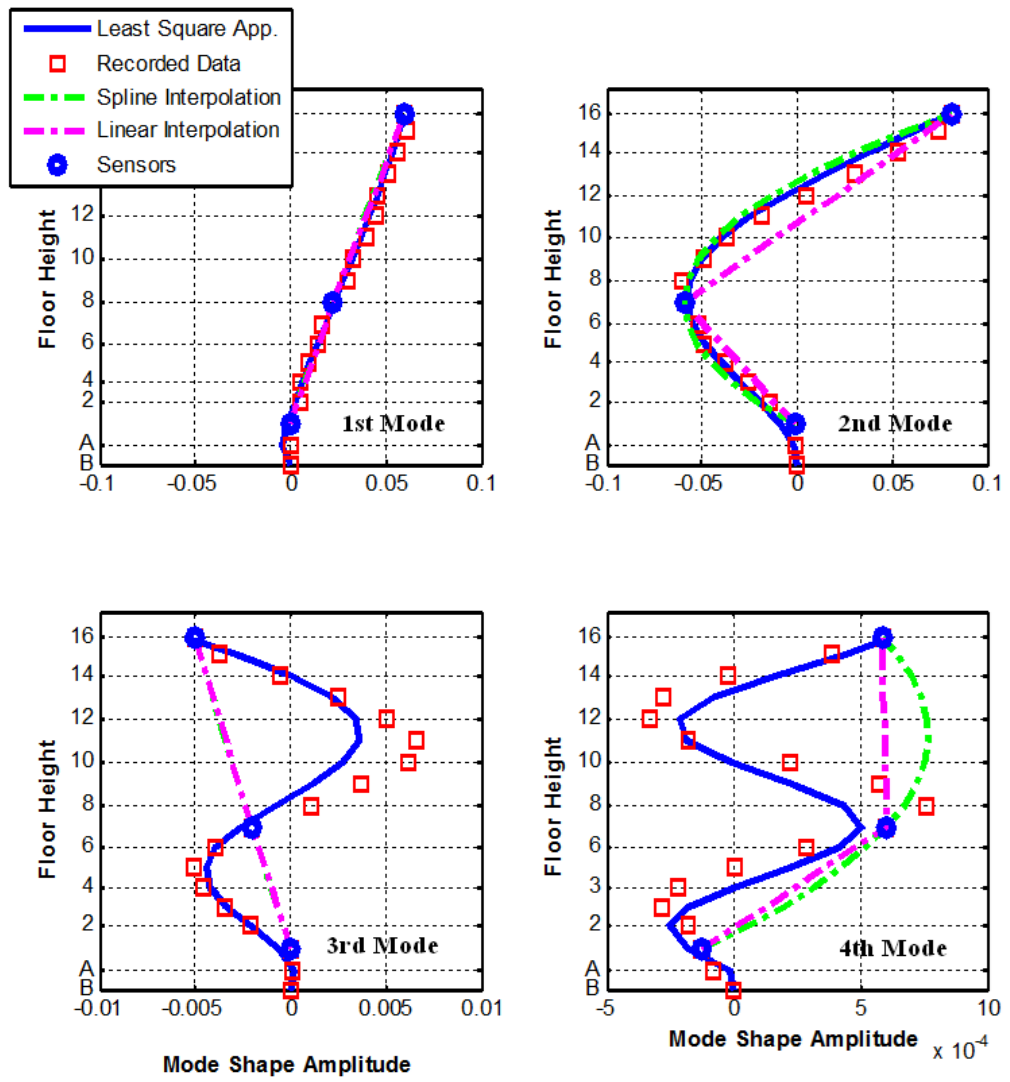
Figure 3.19. Amplitudes of the recorded and estimated mode shapes for the C1 sensor configuration. Blue lines represent the estimated mode shapes using MSBE method, while red squares are the recorded mode shapes.The dashed green and pink lines show the spline and linear interpolations, respectively.
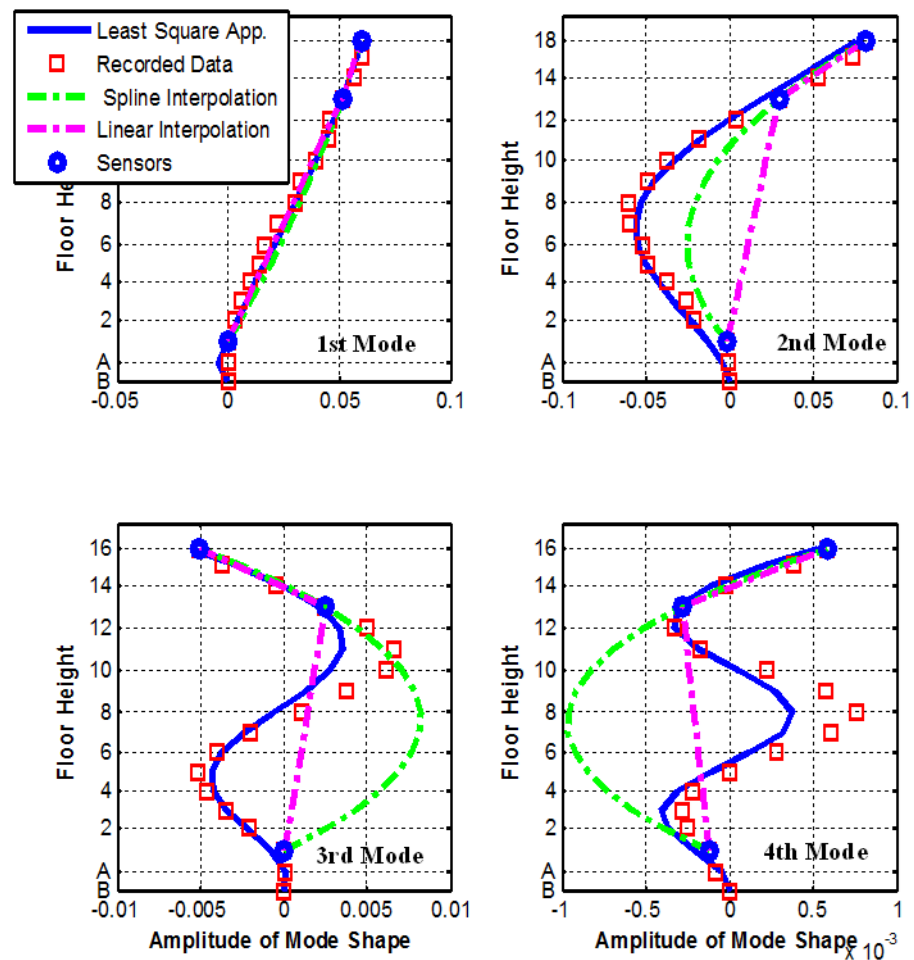
Figure 3.20. Amplitudes of the recorded and estimated mode shapes for the C2 sensor configuration. Blue lines represent the estimated mode shapes using MSBE method, while red squares are the recorded mode shapes.The dashed green and pink lines show the spline and linear interpolations, respectively.

As expected, in both sensor configurations, the MSBE, cubic spline and linear interpolation methods all give a good estimation of the first mode shape, since it is closer to a straight line.

For the second mode, the spline and linear interpolation methods underestimate the modal displacements for floor levels above and below the middle sensor, while the MSBE method gives better estimation for both configurations. The spline interpolation performs better than linear interpolation.

For the third and fourth mode shapes, the linear and spline interpolation methods fail to give a good estimation of the modal amplitudes in both sensor configurations, while the MSBE method provides a reasonably good estimation. This is mainly because of the more frequent change of the sign of the slope in higher modes along the height of the structure. Mode shapes of a multi-story building can usually be divided into several linear segments between points where the slope changes its sign. Therefore, unless one middle sensor is placed at each of these locations (*e.g.*, the 8th floor level for the second mode shape; or the 4th and the 11th floor levels for the 3rd mode shape), linear and cubic spline interpolation methods will always fail to give a good estimation of the amplitudes in higher modes.

In order to have a reasonable good estimation from the interpolation methods, a sensor has to be placed at each level where the sign of the slope changes. In other words, more sensors are needed for the interpolation methods to accurately capture the higher mode shapes. This is not the case for the MSBE method, because it does not interpolate the recorded data at instrumented floors over the height of the building. Instead, it uses the combination of mode shapes of shear and bending beams to provide the best-fit mode shape in a least square sense with minimum instrumentation.

It is clear from Figures 3.19 and 3.20 that the MSBE method has advantages over both interpolation methods at higher modes. It also holds true for the cases where there is minimum instrumentation. The utilization of the MSBE method becomes important when the modal participation factor for higher modes are significant (*e.g.*, tall buildings), since the contribution of a mode to total response is proportional to the modal participation factor as shown in Equation 3.13. Therefore, the more mode-shapes with significant modal participation factors contribute to total response, the more accurate the MSBE method. Only four modes of the Factor building are considered in Equation 3.24.

Figures from 3.21 to 3.24 show the comparison of the recorded and the calculated total displacements at the 4th and 10th floors for the C1 and C2 sensor configurations, respectively. Even tough, the MSBE method slightly underestimates the recorded motions at the instrumented floors; the calculated total displacements are still in very good agreement with the recorded motions at the 4nd and 10th floors.

Figure 3.21. Comparison of recorded and calculated displacement time histories for C1 configuration at 10th floor. a) The MSBE, b) linear interpolation and c) cubic spline interpolation methods.

Figure 3.22. Comparison of recorded and calculated displacement time histories for C1 configuration at 4th floor. a) The MSBE, b) linear interpolation and c) cubic spline interpolation methods.
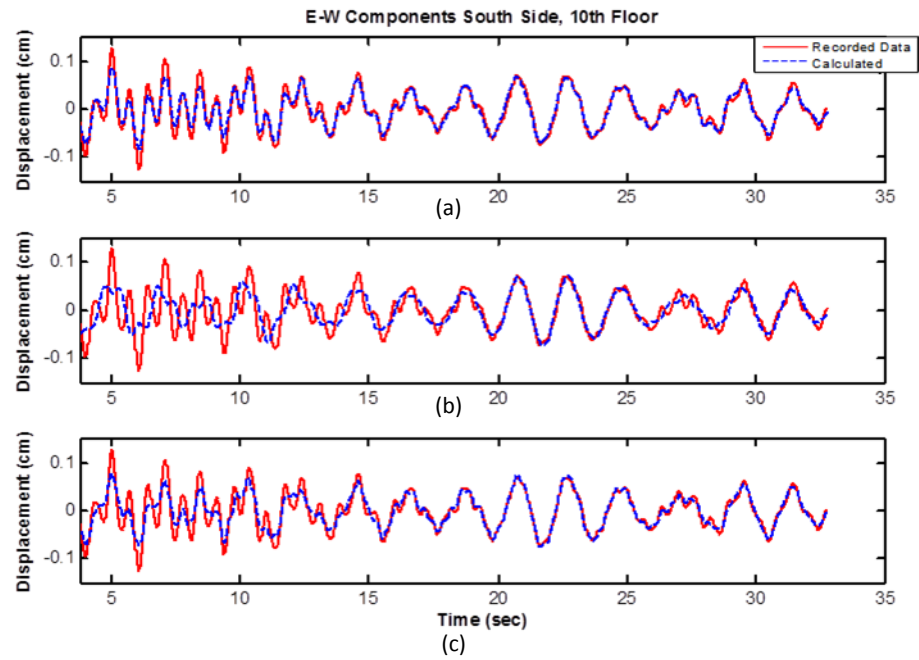
Figure 3.23. Comparison of recorded and calculated displacement time histories for C2 configuration at 10th floor. a) The MSBE, b) linear interpolation and c) cubic spline interpolation methods.
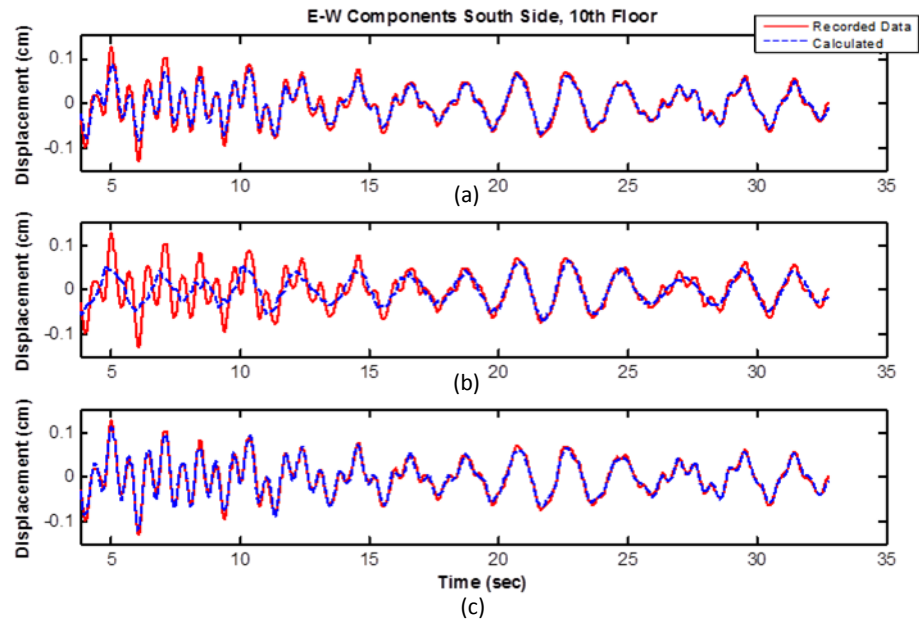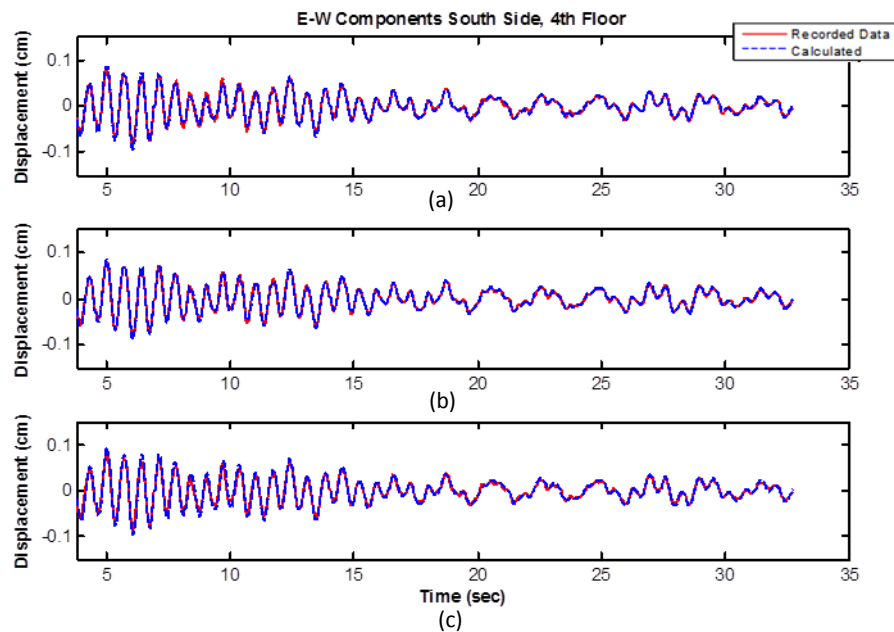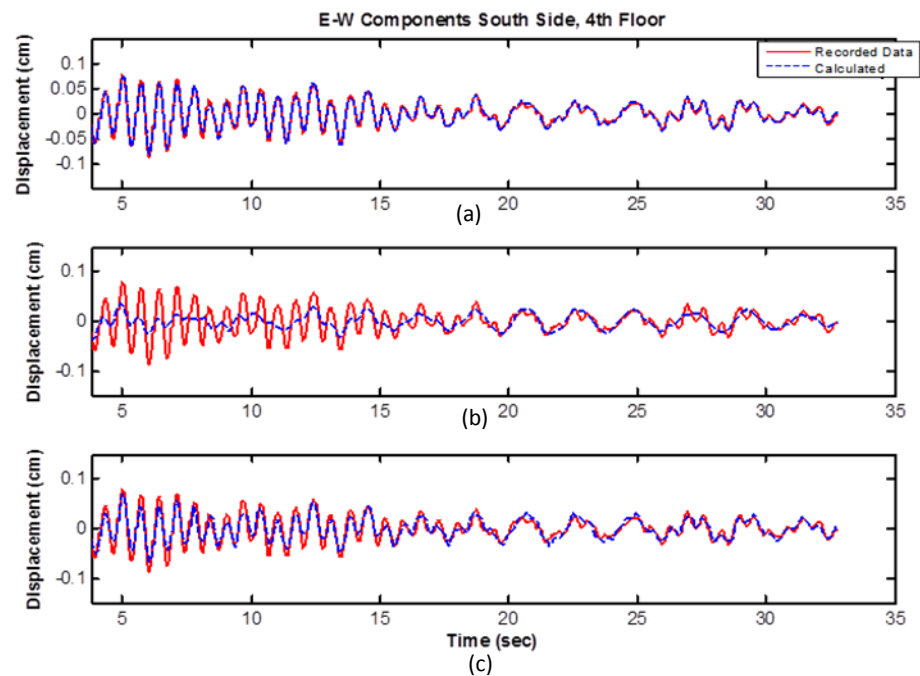

Figure 3.24. Comparison of recorded and calculated displacement time histories for C2 configuration at 4th floor. a) The MSBE, b) linear interpolation and c) cubic spline interpolation methods.

According to above results, it is clear that the MSBE method gives a better estimation of the response than the linear and cubic spline polynomial interpolation methods.

3.4.2. The Robert A. Millikan Library

The accuracy of the MSBE method has also been tested by using earthquake records from for the Millikan Library, which is another building with sensors at every floor.

The Millikan Library has been instrumented and studied since 1966 (Kuroiwa, 1967; Trifunac, 1972; Udwadia and Trifunac, 1974; Luco *et al.*, 1987; Foutch, 1976; Foutch and Jennings, 1978; Chopra, 1995). Clinton (2006) summarize the data collected from the Millikan Library under forced and ambient vibrations, as well earthquakes.

3.4.2.1. Structural Description and Instrumentation. The Robert A. Millikan Library located on the campus of California Institute of Technology in Pasadena, California. The Library is a nine-story reinforced concrete building with a basement. The building is 21.0 m by 22.9 m in plan, and extends 43.9 m above grade, and 48.2 m above the basement level. The building has reinforced-concrete moment-resisting frames in both E-W and N-S directions. There are shear walls on the East and West sides of the building that provide most of the stiffness in the north-south direction (Bradford, 2006). Shear walls in the central core provide added stiffness in the east-west direction. More detailed descriptions of the structural system can be found in Kuroiwa (1967), Foutch *et al.* (1975), Foutch (1976), Luco *et al.* (1987), and Clinton (2006).

Millikan Library was first instrumented in 1968 with two permanent tri-axial accelerometers located on the roof and the basement. After the 1994 Northridge, California Earthquake, the instrumentation was enhanced to 36-channel, real-time system with three horizontals at each floor and three verticals in the basement.

(a)   (b)
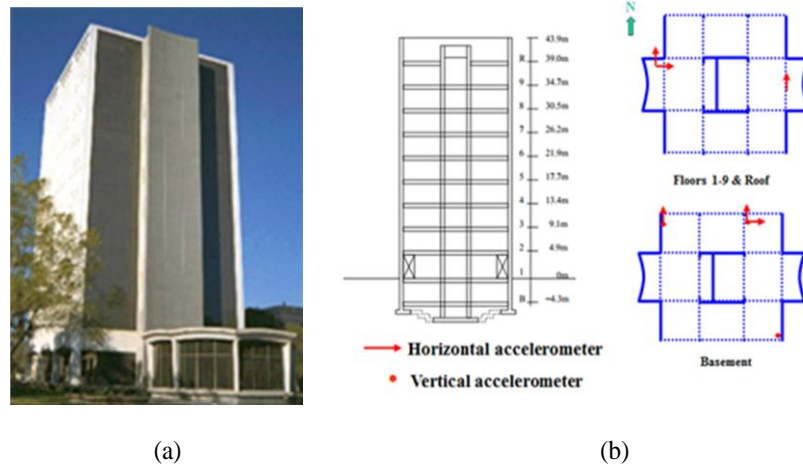
Figure 3.25. (a) North-west side of The Millikan Library (b) Sensor layout of the structure and arrows show the polarities of sensors on each floor.

3.4.2.2. Selected Earthquake Data. To test the accuracy of the MSBE method on the Robert A. Millikan Library, we have used data from M=4.8 Yorba Linda, California Earthquake of 3 September 2002 (Figure 3.26). The epicentral distance of the earthquake from the building was 40 km.
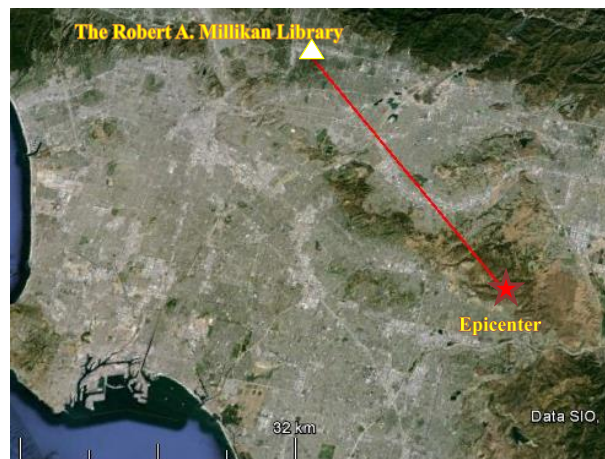
Figure 3.26. Map showing the location of the epicenter of Yorba Linda Earthquake and the Robert A. Millikan Library.

3.4.2.3. Identification of Modal Properties and Application of the MSBE Method. Again, although the building had sensors at every floor, we considered two configurations, assuming only three floors had sensors, to test the accuracy of the MSBE method: Configuration C1 with sensors at 1st and 7th floors, and the roof; and Configuration C2 with sensors at 1st and 5th floors, and the roof. Fourier Amplitude Spectra of the records from the instrumented floors are plotted in Figures 3.27 and 3.28 for the C1 and C2 configurations, respectively. The identified modal frequencies are given in Table 3.3.
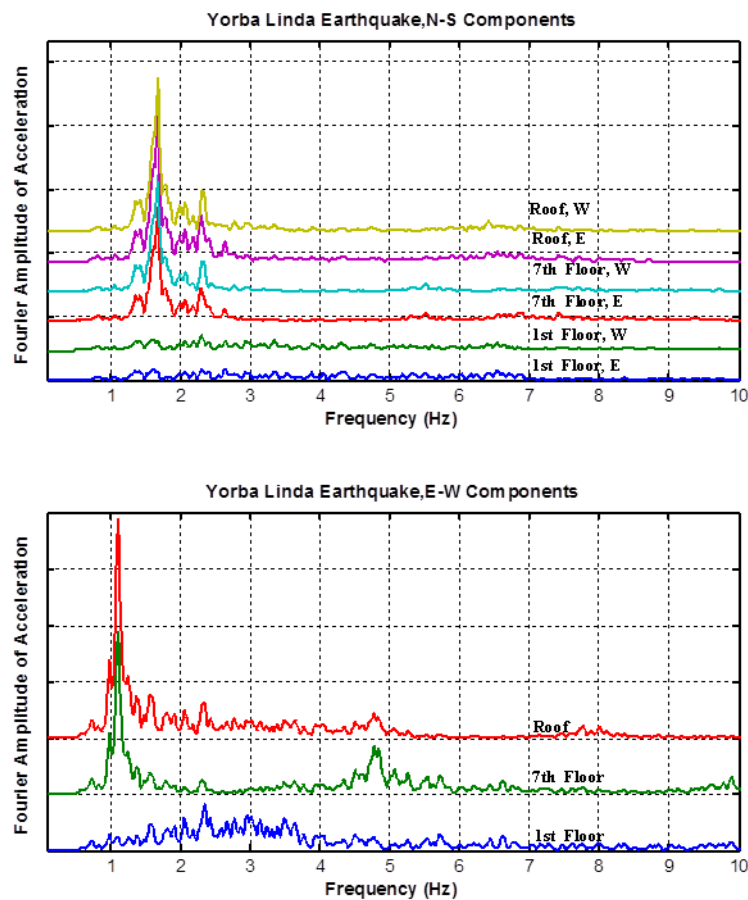
Figure 3.27. Smoothed Fourier Amplitude Spectrum of the Yorba Linda Earthquake, records for the C1 configuration. (a) North-south direction accelerations (b) East-west direction accelerations.
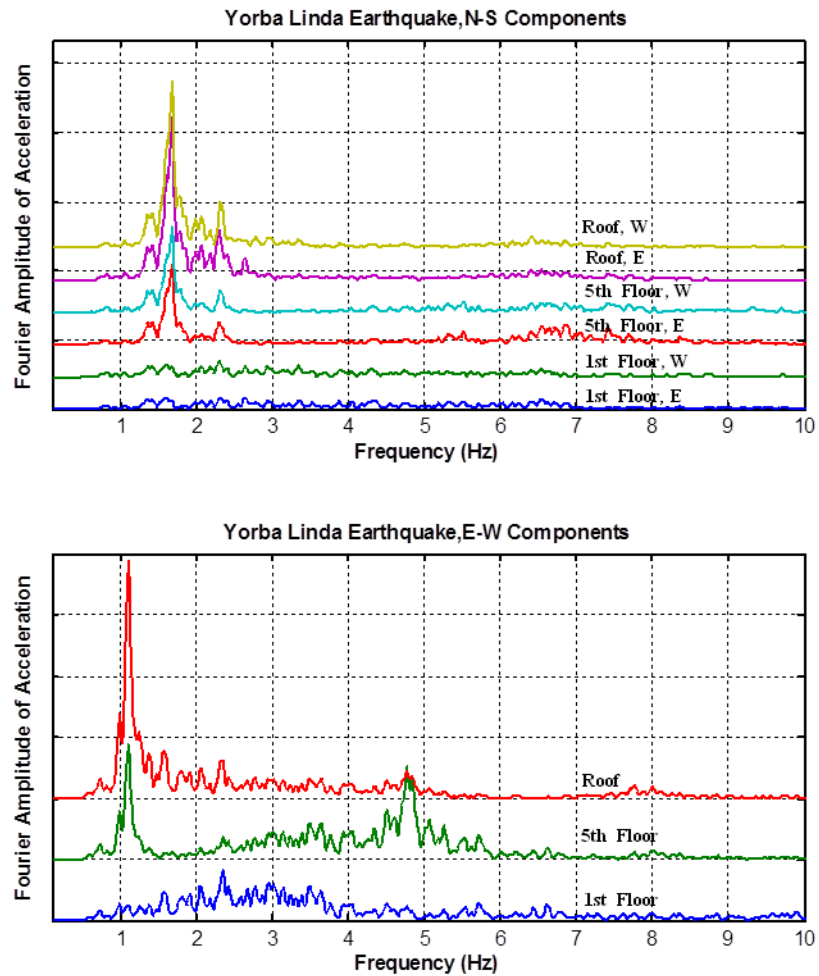
Figure 3.28. Smoothed Fourier Amplitude Spectrum of the Yorba Linda Earthquake, records for the C2 configuration. (a) North-south direction accelerations (b) East-west direction accelerations.

Table 3.3. Modal frequencies of the Millikan Library.

	First Mode (Hz)	Second Mode (Hz)
East-West	1.11	4.7-4.9
North-South	1.6-1.7	6.5-6.9

To test the MSBE method, acceleration time histories are bandpass filtered around the identified modal frequencies and then double integrated to obtain modal displacement time histories. Figures 3.29 and 3.30 show the recorded first two-mode shapes of Millikan Library that are calculated by using records from all the floors, and their match by the

mode shapes approximated, based on the records from only three floors, by using the MSBE method and the linear and cubic interpolations for the sensor configurations C1 and C2. The figures are given for the East-West components of the records only.
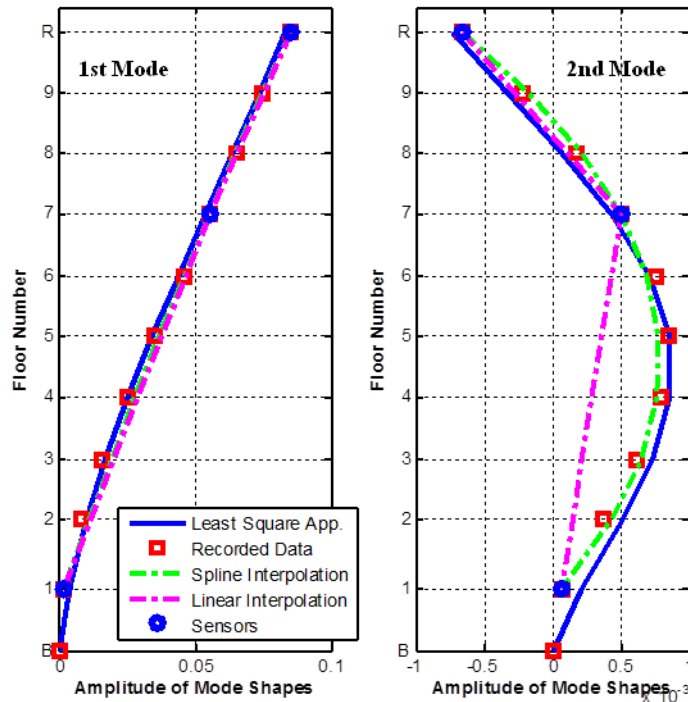
Figure 3.29. Amplitudes of the identified and estimated mode shapes for the C1 sensor configuration: Blue lines represent the estimated mode shapes using the MSBE method; red squares denote the recorded mode shape; and the dashed green and pink lines show the spline and linear interpolations, respectively.
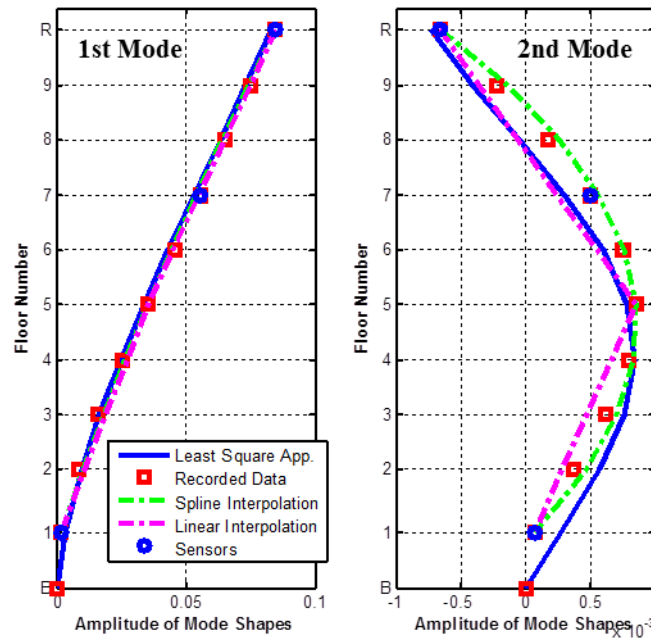
Figure 3.30. Amplitudes of the identified and estimated mode shapes for the C2 sensor configuration: Blue lines represent the estimated mode shapes using the MSBE method; red squares denote the recorded mode shape; and the dashed green and pink lines show the spline and linear interpolations, respectively.

Since the first mode shape of the building is closer to a straight line, all three methods give a good estimation of the first mode shape in both sensor configurations. The second mode shape is badly matched by the linear interpolation. Again, the location of the middle sensor is the key to the accuracy of the interpolation approaches.

Figures from 3.31 to 3.34 show the comparison of the recorded and calculated total displacements of the 4th and the 9th floors for the C1 and C2 sensor configurations, respectively. Even tough, the MSBE method slightly underestimates the recorded motion at instrumented floors; the calculated total displacements are still in very good agreement with the recorded motions at the 4nd and 9th floors.
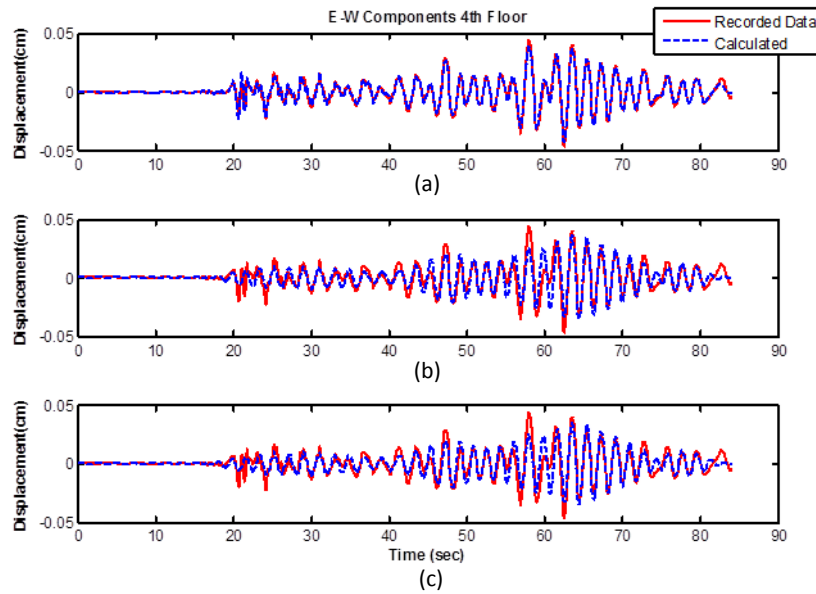
Figure 3.31. Comparison of recorded and calculated displacement time histories for C1 configuration at 4th floor. a) The MSBE, b) linear interpolation and c) cubic spline interpolation methods.
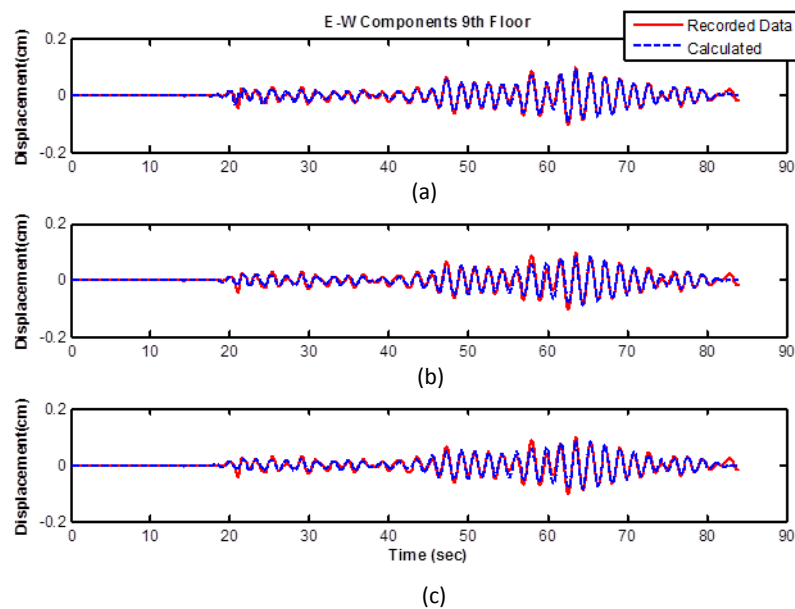
Figure 3.32. Comparison of recorded and calculated displacement time histories for C1 configuration at 9th floor. a) The MSBE, b) linear interpolation and c) cubic spline interpolation methods.
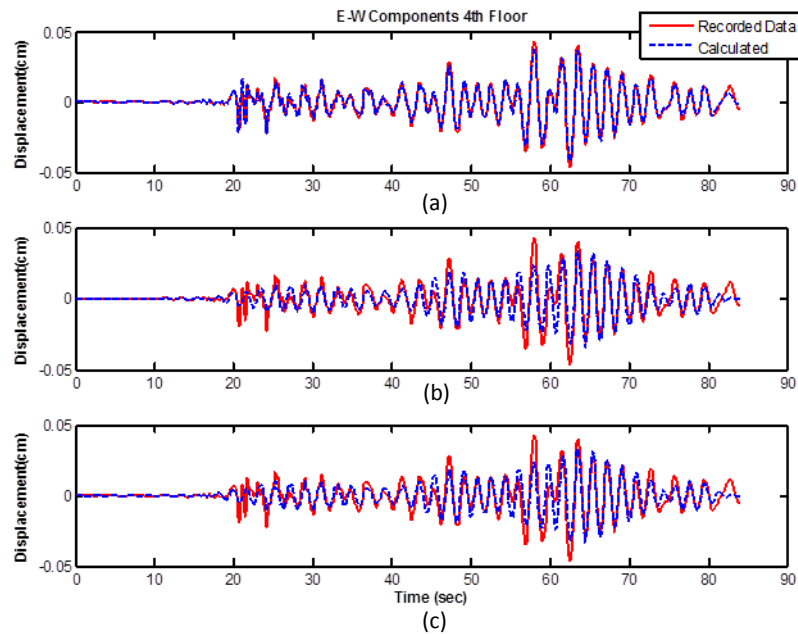
Figure 3.33. Comparison of recorded and calculated displacement time histories for C2 configuration at 4th floor. a) The MSBE, b) linear interpolation and c) cubic spline interpolation methods.
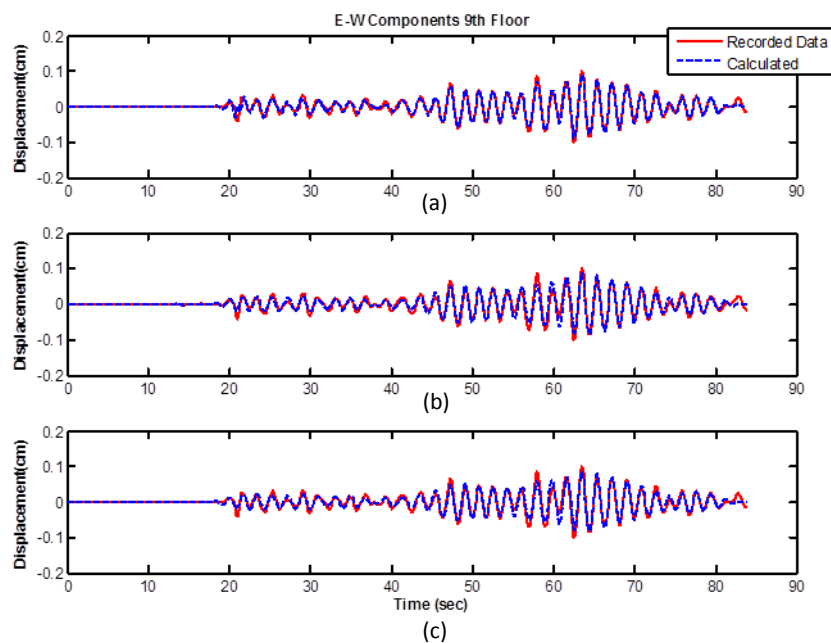
Figure 3.34. Comparison of recorded and calculated displacement time histories for C2 configuration at 9th floor. a) The MSBE, b) linear interpolation and c) cubic spline interpolation methods.

4. DEVELOPMENT OF ANALYTICAL MODELS FROM VIBRATION RECORDS

One of the advantages of knowing vibration time histories at all the floors of a multi-story building is that more accurate analytical models of the building can be developed. For multi-storey buildings, analytical models are usually developed from earthquake records by matching the modal characteristics (*i.e.,* modal frequencies, damping ratios, mode shapes) of the data and the model. However, as mentioned in Chapter 1, records are available usually at a limited number of floors and calibration of analytical models by using limited data can cause non-unique results. In other words, more than one model can match the modal properties of the structure with the data.

It can also be shown that modal properties are not very sensitive to the changes in structural properties. As an example, we study the sensitivity of the natural frequencies of a building to the changes in one of the story stiffness's. Consider a 10-story building with the following properties: $m_i = 12x10^4$ kg and $k_i = 20.504x10^7$ N/m for all the stories, and the damping is assumed to be Rayleigh damping. The damping ratios for the first two modes are 2%. To investigate the sensitivity of modal frequencies to a structural parameter, we gradually reduced the 6th story stiffness down to 10% of its original value with 10% increments, and observed the changes in structural frequencies. Figure 4.1 shows the per cent changes in the first three modal frequencies of the structure with percent reduction in the 6th story stiffness.
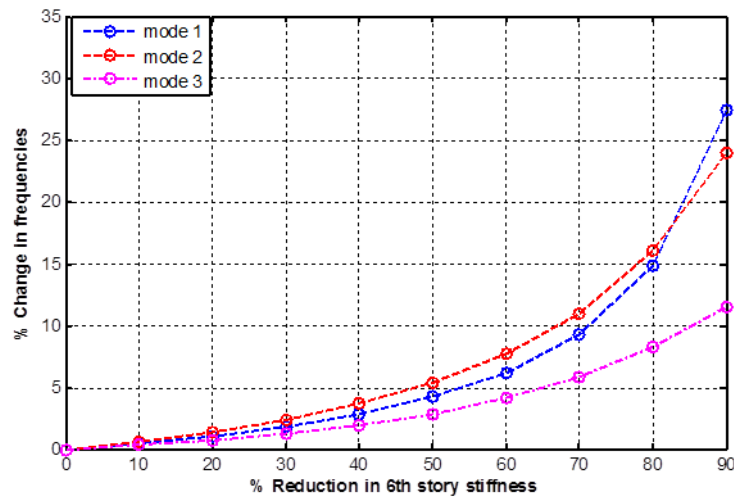
Figure 4.1. Comparison of percent changes in first three frequencies of the structure with per cent reduction in the 6th story stiffness.

Figure 4.1 clearly shows that first two modes are more sensitive to the change, and in order to see a 5% reduction in these frequencies, more than 50% reduction in the 6th story stiffness is required. Experiments with stiffness changes in other stories gave similar results. Therefore, it can be concluded that modal frequencies are not a good indicator of damage, because large reductions in story stiffnesses are required to see any significant change in modal frequencies.

As an alternative to matching modal properties, we will present a calibration method for multi-storey buildings based on the transfer matrix formulation of the response. The method requires that the vibration time histories of the building are measured or estimated at every floor.

The Transfer Matrix method, also known as the Holzer's Method, is an alternative approach to study the dynamic response of chain-type structures, such as multi-story buildings (Clough and Penzien, 1975). A transfer matrix gives the relationship between the forces and displacements in two adjacent sections of chain-like structures. The complete force and displacement relationship between any two points of the structure can be obtained through a sequence of transfer matrices. With this approach, a large system is separated into simple subsystems.

A brief description of the transfer matrix method for an *N*-story shear building is discussed below. Consider an *N-story* shear building excited by ground acceleration $\ddot{x}_g(t)$, as shown in Figure 4.2. Forces and displacements that define the motions of two adjacent floors, floors *i* and *i+1*, are shown in Figure 4.3, where *y* represents the displacement relative to the base of the building and $f_i = -m_i \ddot{x}_g$, the inertial load due to base acceleration. For the moment, we are neglecting the damping forces for simplicity in the formulation.
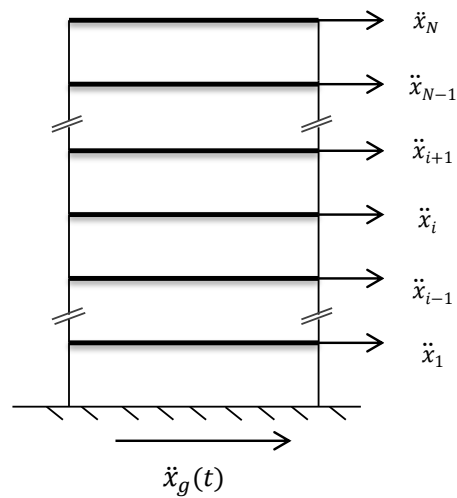
Figure 4.2. An *N-story* shear building under base excitation $\ddot{x}_g(t)$.
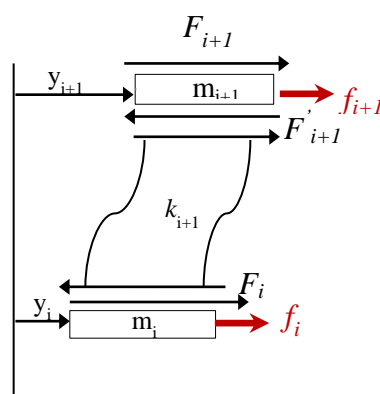
Figure 4.3. Forces and displacements for two adjacent floors.

From the equilibrium of the forces acting on the floor mass m_{i+1}, we can write:

$$m_{i+1}\ddot{y}_{i+1} = F_{i+1} - F'_{i+1} + f_{i+1} \qquad (4.1)$$

where $f_{i+1} = -m_{i+1} \cdot \ddot{x}_g$, and a dot over a variable denotes the derivative with respect to time. F_{i+1} and F'_{i+1} represent the internal forces above and below the mass $i+1$, respectively. Since the displacement on either side of m_{i+1} is the same, we can also write:

$$y_{i+1} = y'_{i+1} \qquad (4.2)$$

where y_{i+1} and y'_{i+1} denote the displacements, relative with respect to base, above and below the mass $i+1$, respectively. By using Equations 4.1 and 4.2, and also noting that for a harmonic excitation with frequency ω, $\ddot{y}_{i+1} = -\omega^2 y_{i+1}$, we can write the following matrix equation (*i.e.*, the *point matrix*) for level $i+1$:

$$\begin{bmatrix} y_{i+1} \\ F_{i+1} \end{bmatrix} = \begin{bmatrix} 1 & 0 \\ -\omega^2 m_{i+1} & 1 \end{bmatrix} \begin{bmatrix} y'_{i+1} \\ F'_{i+1} \end{bmatrix} + \begin{bmatrix} 0 \\ m_{i+1} \cdot \ddot{x}_g \end{bmatrix} \qquad (4.3)$$

From the equilibrium of the forces acting on the segment between the two floors, we can write: $F'_{i+1} = F_i$. These forces are generated by the relative motions between floors i and $i+1$, and are equal to

$$F'_{i+1} = F_i = k_{i+1}(y'_{i+1} - y_i) \qquad (4.4)$$

where k_{i+1} is the stiffness of the $i+1$'th story. Equation 4.4 can be put into the following matrix form (*i.e.*, the *field matrix*):

$$\begin{bmatrix} y'_{i+1} \\ F'_{i+1} \end{bmatrix} = \begin{bmatrix} 1 & 1/k_{i+1} \\ 0 & 1 \end{bmatrix} \begin{bmatrix} y_i \\ F_i \end{bmatrix} \qquad (4.5)$$

By inserting Equation 4.5 in Equation 4.3 we can write the following transfer matrix equation for the transfer of displacements and forces from floor i to floor $i+1$:

$$\begin{bmatrix} y_{i+1} \\ F_{i+1} \end{bmatrix} = \begin{bmatrix} 1 & 0 \\ -\omega^2 m_{i+1} & 1 \end{bmatrix} \begin{bmatrix} 1 & 1/k_{i+1} \\ 0 & 1 \end{bmatrix} \begin{bmatrix} y_i \\ F_i \end{bmatrix} + \begin{bmatrix} 0 \\ m_{i+1} \cdot \ddot{x}_g \end{bmatrix} \qquad (4.6a)$$

$$\begin{bmatrix} y_{i+1} \\ F_{i+1} \end{bmatrix} = \begin{bmatrix} 1 & 1/k_{i+1} \\ -\omega^2 m_{i+1} & 1 - \omega^2/\omega_{i+1}^2 \end{bmatrix} \begin{bmatrix} y_i \\ F_i \end{bmatrix} + \begin{bmatrix} 0 \\ m_{i+1} \cdot \ddot{x}_g \end{bmatrix} \qquad (4.6b)$$

where $\omega_{i+1}^2 = k_{i+1}/m_{i+1}$.

Note that, for the top story (*i.e.*, *i+1=N*): $F_N=0$. Thus, Equation 4.6 for the top story becomes:

$$y_N = y_{N-1} + \frac{F_{N-1}}{k_N} \qquad (4.7a)$$

$$0 = m_N\left(-\omega^2 y_{N-1} + \ddot{x}_g\right) + (1 - \frac{\omega^2}{\omega_N^2})F_{N-1} \qquad (4.7b)$$

Let x_i denote the total displacement of the *i*'th floor (*i.e.*, $x_i = y_i + x_g$) and note that $-\omega^2 y_{N-1} + \ddot{x}_g = \ddot{x}_{N-1}$. by extracting F_{N-1} from Equation 4.7b, and inserting it in Equation 4.7a, we get the following for F_{N-1}, and the ratio of the total displacements, x_N / x_{N-1}:

$$F_{N-1} = \frac{k_N \ddot{x}_N}{\omega^2 - \omega_N^2} \qquad (4.8a)$$

$$\frac{x_N}{x_{N-1}} = \frac{\omega_N^2}{\omega_N^2 - \omega^2} \qquad (4.8b)$$

This ratio Equation 4.8b is also valid for the corresponding total velocities and accelerations, as well as their Fourier Amplitude Spectra. Thus, we can write for the spectral ratio, $SR_N(\omega)$, of total accelerations at the top two floors:

$$SR_N(\omega) = \frac{|\ddot{X}_N(\omega)|}{|\ddot{X}_{N-1}(\omega)|} = \frac{\omega_N^2}{\omega_N^2 - \omega^2} \qquad (4.9a)$$

Equation 4.9a shows that the spectral ratio of the total accelerations for the top two floors is a function of the individual frequency ω_N of the top floor (*i.e.*, $\omega_N^2 = k_N/m_N$),

and has its peak at $\omega=\omega_N$ (*i.e.*, by making the denominator equal to zero). It is not influenced by the dynamic characteristics of the stories below, as well as the excitation. Thus, by taking the spectral ratio of accelerations recorded at floors *N* and *N-1*, we can determine the natural frequency of the top floor, and consequently the stiffness of the top floor (assuming that the mass of the top floor is known or estimated).

If we include damping, Equation 4.9a takes the following form (Şafak, 1995):

$$[SR_N(\omega)]^2 = \frac{\omega_N^4 + (2\xi_N\omega_N\omega)^2}{(\omega_N^2 - \omega^2)^2 + (2\xi_N\omega_N\omega)^2} \tag{4.9b}$$

where ξ_N is the damping ratio for the *N*'th floor (*i.e.*, $\xi_N=c_N/(2m_N\omega_N)$). It can be shown, by making the derivative of Equation 4.9b with respect to ω equal to zero, that $SR_N(\omega)$ has its peak at frequency ω_{max}, which is given by (Şafak, 1995)

$$\omega_{max} = \frac{\left[-1 + \sqrt{1 + 8\xi_N^2}\right]^{1/2}}{2\xi_N}\omega_N \tag{4.9c}$$

For low damping values (*e.g.*, $\xi < 0.30$), the coefficient of ω_N on the right hand side is close to 1.0 and it can be approximated that $\omega_{max}\approx\omega_N$.

We can write Equations 4.7a and 4.7b for the next floor, floor *N-1*, similarly. By replacing, the subscripts *N* and *N-1* with *N-1* and *N-2*, respectively, and also noting that the left-hand side of Equation 4.7b is no longer zero, the equations for the *N-1*'th floor become:

$$y_{N-1} = y_{N-2} + \frac{F_{N-2}}{k_{N-1}} \tag{4.10a}$$

$$F_{N-1} = m_{N-1}(-\omega^2 y_{N-2} + \ddot{x}_g) + (1 - \frac{\omega^2}{\omega_{N-1}^2})F_{N-2} \tag{4.10b}$$

By extracting F_{N-2} from Equation 4.10b and inserting it in Equation 4.10a, and also using the values of F_{N-1} and $\ddot{x}_N$ from Equations 4.8a and 4.8b, we can show that the ratio

$|\ddot{X}_{N-1}(\omega)|/|\ddot{X}_{N-2}(\omega)|$ is a function of the properties of stories *N* and *N-1* only (*i.e.*, function of $\omega_N^2 = \frac{k_N}{m_N}$, $\omega_{N-1}^2 = \frac{k_{N-1}}{m_{N-1}}$, and m_N/m_{N-1}). Again, this ratio is a function of the physical properties of the story *N-1* and the stories above; it does not depend on the properties of the stories below. Since we have already determined ω_N and k_N earlier from the spectral ratio $X_N(\omega)/X_{N-1}(\omega)$, we can now determine ω_{N-1} and k_{N-1} from the spectral ratio $X_{N-1}(\omega)/X_{N-2}(\omega)$ (again, we are assuming that the mass m_{N-1} is known or estimated). We keep doing this until we cover all the stories.

To demonstrate this concept, a numerical example is presented below. Consider the ten-story building that is used earlier (Figure 4.2). We computed the seismic response of the building twice, first assuming no damage (*i.e.*, the original stiffness values), and next by reducing the 5th story stiffness by 50%. We used one of the acceleration records from the M=7.4, 17 August 1999 Kocaeli Earthquake as the ground motion. The modal frequencies for the undamaged and damaged cases are given in Table 4.1 and Figure 4.4 presents the comparison of spectral ratios of successive floors for the undamaged and damaged cases. As clearly seen from the figure, the stiffness change on the 5th story changes the spectral ratios only for the 5th story and the stories below. The ratios for the stories above do not change. Therefore, any adjustment at a story stiffness made by using spectral ratios does not have any effect on the spectral ratios for the stories above. Note that this does not mean the responses of the stories above do not change, but only their ratios. Thus, we can start the model calibration from the top story, knowing that the calibration of the stories below will not change the calibrations already made for the stories above.

Table 4.1. Modal frequencies of the 10-story building before and after damage on 5th story.

Mode Number	Modal Frequency		
	Undamaged (Hz)	Damaged (Hz)	Difference (%)
1	0.9833	0.9298	5.4
2	2.9279	2.8755	1.8
3	4.8071	4.4334	7.8
4	6.5789	6.5789	-
5	8.2037	7.6003	7.4
6	9.6453	9.5111	1.4
7	10.8714	10.4199	4.2
8	11.8547	11.5322	2.7
9	12.5732	12.4369	1.1
10	13.0108	12.7486	2.0

The calibration approach presented above can also be used for damage detection and damage location in multi-story buildings from their earthquake records. By comparing the spectral ratios of adjacent floors that are calculated from the pre- and post-earthquake records, the stories with stiffness changes can easily be identified.
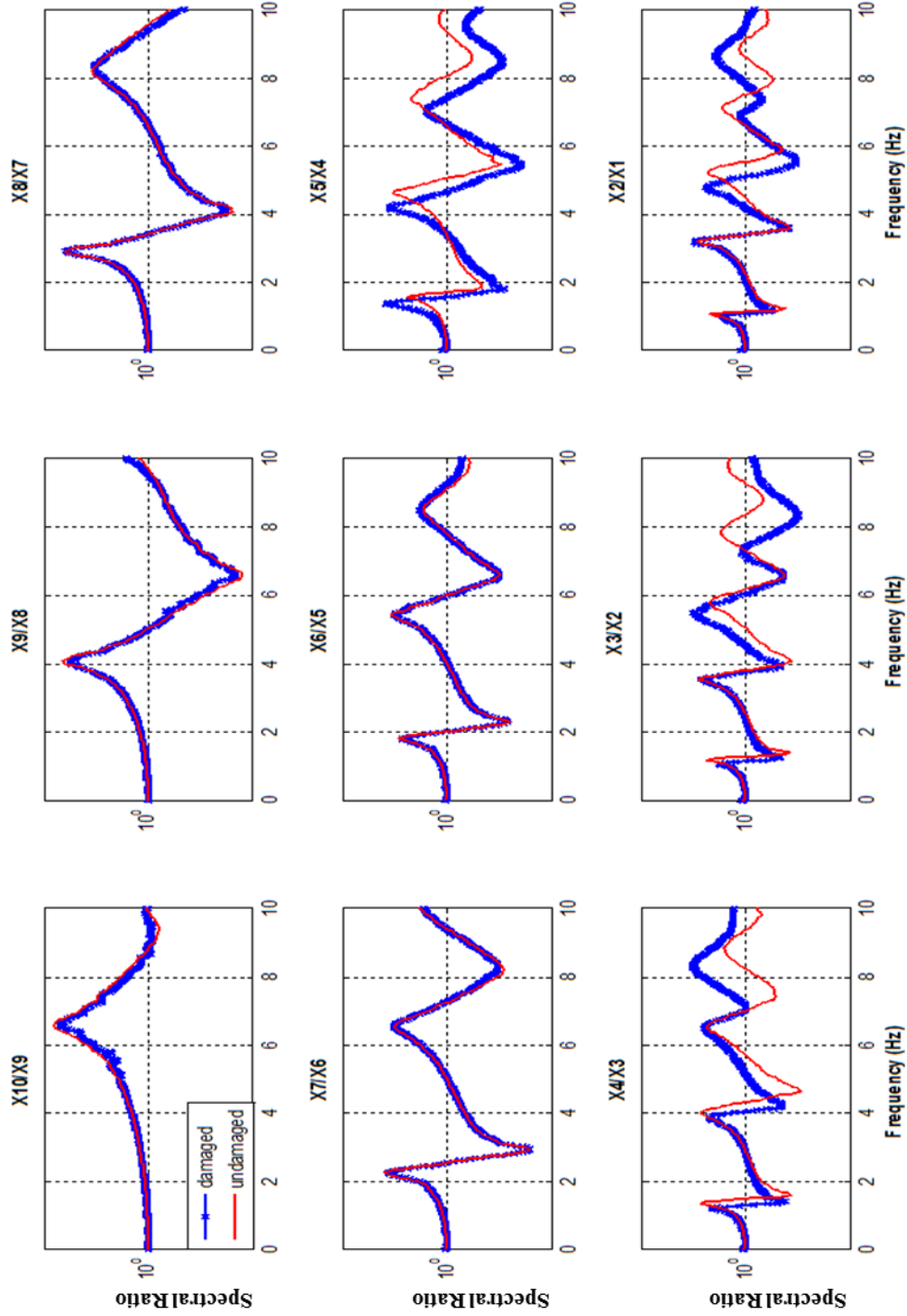
Figure 4.4. Spectral Ratios for 10 story shear building with and without damage at 5th story.

5. CONCLUSION

Analytical models of multi-story buildings can be calibrated uniquely by using vibration records taken from only a few floors. The first step in the calibration is to estimate vibration time histories at the non-instrumented floors. This is done by assuming that each mode shape of the building can be approximated as a linear combination of mode shapes of a shear beam and a bending beam.

Once the vibration time histories are known at every floor, the story stiffnesses can be determined uniquely by matching the dominant frequencies of the top-to-bottom spectral-ratios at each story. The spectral ratio of a story is not influenced by any structural changes in the stories below. Therefore, the calibration has to start from the top story.

Numerical examples by using real and simulated records confirm the validity and the superiority of the approach.

REFERENCES

Beck, J. L., and L. S. Katafygiotis, 1998, "Updating Models and Their Uncertainties. I: Bayesian Statistical Framework", *Journal of Engineering Mechanics*, Vol. 124, No. 4, pp. 455-561.

Bradford, S. C., 2006, *Time-Frequency Analysis of Systems with Changing Dynamic Properties*, Ph.D., Dissertation, California Institute of Technology.

Carden, E.P., and P. Fanning, 2004, "Vibration-Based Condition Monitoring- A review", *Structural Health Monitoring*, Vol. 3, No. 4, pp. 355-377.

Chang, P.C., A. Flatau, and S.C. Liu, 2003, "Review Paper: Health Monitoring of Civil Infrastructure", *Structural Health Monitoring*, Vol. 2, No. 3, pp. 257-267.

Chopra, A.K., 2007, "Dynamics of Structures: Theory and Applications to Earthquake Engineering", *Prentice-Hall,* Upper Saddle River, USA.

Clough, R.W., and J. Penzien, 1993, "Dynamics of Structures", 2n Edition, *McGraw-Hill*, New York, N.Y.

Clinton, J.F., S.C. Bradford, T.H. Heaton, and J. Favela, 2006, "The Observed Wander of the Natural Frequencies in A structure", *Bulletin of the Seismological Society of America*, Vol. 96, No.1, pp. 237-257.

De la Llera J. C. and A.K. Chopra, 1997, "Evaluation of Seismic Code Provisions Using Strong-Motion Building Records from the 1994 Northridge Earthquake", *Report UCB/EERC-97/16*, University of California, Berkeley, USA.

Doebling, S.W., C.R. Farrar, M.B. Prime and D.W. Shevitz, 1996, "Damage Identification and Health Monitoring of Structural and Mechanical Systems from Changes in Their

Vibration Characteristics: A Literature Review", *Los Alamos National Laboratory Report*, LA-13070-MS.

Foutch, D.A., 1976, *A Study of the Vibrational Characteristics of Two Multistorey Buildings*., Ph.D., Dissertation, California Institute of Technology, Earthquake Research Laboratory, Pasadena, California.

Foutch, D.A., and P.C. Jennings, 1978, "A Study of the Apparent Change in the Foundation Response of a Nine –Story Reinforced Concrete Building", *Bulletin of the Seismological Society of America*, Vol. 68, No.1, pp. 219-229.

Goel, R.K., 2005, "Evaluation of Modal and FEMA Pushover Procedures Using Strong-Motion Records of Buildings", *Earthquake Spectra,* Vol. 21, No.3, pp. 653-684.

Goel, R.K., 2008, "Mode-Based Procedure to Interpolate Strong Motion Records of Instrumented Buildings", *ISET Journal of Earthquake Technology,* Vol. 45, No. 3-4, pp. 97-113.

Iwan, W., 1997, "Drift Spectrum: Measure of demand for Earthquake Ground Motion", *Journal of Structural Engineering*, Vol. 123, No.4, pp. 397-404.

Jennings, R.L., and N.M. Newmark, 1960, "Elastic Response of Multi-Story Shear Beam type Structures Subjected to Strong Ground Motion", *Proceedings of the Second World Conference on Earthquake Engineering*, Vol 2, Science Council of Japan, Tokyo, Japan.

Jennings, P.C., and J. Bielak, 1973, "Dynamics of Building-Soil Interaction", *Bulletin of the Seismological Society of America*, Vol. 63, pp. 9-48.

Kohler, M., P.D. Davis and E. Şafak, 2005, "Earthquake and Ambient Vibration Monitoring of the Steel-Frame UCLA Factor Building", *Earthquake Spectra*, Vol. 21, No.3, pp. 751-736.

Kunnath, S.K., Q. Ngheim, and S. El-Tawii, 2004, "Modeling and Response Prediction in Performance-Based Seismic Evaluation: Case Studies of Instrumented Steel Moment-Frame Buildings", *Earthquake Spectra*, Vol. 20, No. 3, pp. 883-915.

Kuroiwa, J.H., 1967, *Vibration Test of a Multistory Building*., Ph.D., Dissertation, California Institute of Technology, Earthquake Research Laboratory, Pasadena, California.

Lee W. HK., H. Kanamori, P. C. Jennings, and K. Kisslinger, 2003, "International Handbook of Earthquake and Engineering Seismology, Part 2", *Academic Press*.

Limongelli, M.P., 2003, "Optimal Location of Sensors for Reconstruction of Seismic Reponses through Spline Function Interpolation", *Earthquake Engineering and Structural Dynamics*, Vol. 32, No. 7, pp. 1055-1074.

Limongelli, M.P., 2005, "Performance Evaluation of Instrumented Buildings", *ISET Journal of Earthquake Technology*, Vol. 42, No. 2-3, pp. 47-61.

Luco, J.M., M. Trifunac, and H. Wong, 1987, "On the Apparent Change in Dynamic Behavior of a 9-Story Reinforced-Concrete Building", *Bulletin of Seismological Society of America,* Vol. 77, No. 6, pp. 1961-1983.

Mathworks, 2013, "MATLAB- The Language of Technical Computing", *The Math works*, Natick, USA.

Miranda, E., 1999, "Approximate Seismic Lateral Deformation Demands in Multistory Buildings", *Journal of Structural Engineering*, ASCE, Vol. 125, No.4, pp. 417-425.

Miranda, E., and S. Akkar, 2006, "Generalized Interstory Drift Spectrum", ASCE, *Journal of Structural Engineering*, Vol. 132, No. 6, June 1, 2006.

Mottershead, J.E., and M.I. Friswell, 1993, "Model Updating in Structural Dynamics: A Survey", *Journal of Sound and Vibration*, Vol. 167, No.2, pp. 347-375.

Naeim, F., 1997, "Performance of Extensively Instrumented Buildings during the January 17, 1994 Northridge Earthquake: An Interactive Information System", *Jama Report 97-7530.68, John A. Martin and Associates*, Los Angeles, USA.

Naeim, F., H. Lee, H. Bhatia, S. Hegie, and K. Skliros, 2004, "CSMIP Instrumented Building Response Analysis and 3-D Visualization System (CSMIP-3DV)", *Proceedings of the SMIP04 Seminar on Utilization of Strong-Motion Data,* Sacramento, USA, pp. 82-102.

Naeim, F., S. Hagie, H. Bhatia, A. Alimoradi, and E. Miranda, 2006, "Three-Dimensional Analysis, Real-Time Visualization, and Automated Post-Earthquake Damage Assessment of Buildings", *Structural Design Tall Special Buildings,* Vol. 15, pp. 105-138.

Rahmani, M., and M.I. Todorovska, 2014, "1D System Identification of 54-Story Steel Frame Building by Seismic Interferometry", *Earthquake Engineering and Structural Dynamics*, Vol. 43, pp. 627-640.

Skolnik, D., L. Ying, Y. Eunjong, and J.W. Wallace, 2006, "Identification, Model Updating and Response Prediction of an Instrumented 15-Story Steel-Frame Building", *Earthquake Spectra*, Vol. 22, No.3, pp. 781-802.

Sohn, H., C.R. Farrar, F.M. Hemez, D.D. Shunk, D.W. Stinemates, B.R. Nadler, and J.J. Czarnecki, 2004, "A Review of Structural Health Monitoring Literature", *Los Alamos National Laboratory Report,* LA-13976-MS.

Şafak, E., 1995, "Detection and Identification of Soil-Structure Interaction in Buildings from Vibration Recordings", *Journal of Structural Engineering*, Vol. 22, pp. 899-906.

Şafak. E., 2005b, "Detection of Seismic Damage in Structures from Continuous Vibration Records", *Proceedings 9ᵗʰ International Conference on Structural Safety and Reliability*, Rome, Italy.

Şafak, E., and E. Çakti, 2014, "Simple Techniques to Analyze Vibration Records From Buildings", *Proceedings of the 7th European Workshop on Structural Health Monitoring,* 8-11 July 2014, Nantes, France.

Stewart, J.P., and G.L. Fenves, 1998, "System Identification for Evaluating Soil–Structure Interaction Effects in Buildings from Strong Motion Recordings", *Earthquake Engineering and Structural Dynamics*, Vol. 27, pp. 869-885.

Trifunac, M.D., M.I. Todorovska, M.I. Manić and B.D. Bulajić, 2010, "Variability of the Fixed-Based and Soil-Structure System Frequencies of a Building-the Case of Borik-2 Building", *Structural Control Health Monitoring*, Vol. 17, No.2, pp. 120-151.

Trifunac, M.D., 1972, "Comparisons between Ambient and Forced Vibration Experiments", *Earthquake Engineering and Structural Dynamics*, Asce, Vol. 1, pp. 133-155.

Udwadia, F.R., and M.D. Trifunac, 1974, "Time and Amplitude Dependent Response of Structure", *Earthquake Engineering and Structural Dynamics*, Asce, Vol. 2, pp. 359-378.

Westergaard, H.M., 1933, "Earthquake-Shock Transmission in Tall Buildings", *Journal of Structural Engineering*, Asce, Vol. 125, No.4, pp. 417-425.